

^1H NMR (toluene- d_8 , 243 K) 9.71 ppm (d, 1, $^3J_{\text{HP}} = 2.4$ Hz, CHCMe_3), 1.59 (s, 9, OCMe_3), 1.56 (s, 9, OCMe_3), 1.35 (s, 9, CHCMe_3), 0.82 (dt, 9, $^3J_{\text{HH}} = 7.32$ Hz, $^3J_{\text{HP}} = 14.7$ Hz, PCH_2CH_3). The minor isomer has an H_α resonance at ppm 10.58 (d, $^3J_{\text{HP}} = 4.3$ Hz). ^{13}C NMR (toluene- d_8 , 253 K, gated proton decoupled) major isomer 268 (dd, $J_{\text{CH}} = 119$ Hz, $^2J_{\text{CP}} = 6.6$ Hz, CHCMe_3), 77.1 (s, OCMe_3), 75.0 (s, OCMe_3), 42.2 (s, CHCMe_3), 34.2 (q, $J_{\text{CH}} = 125$ Hz, CHCMe_3), 32.7 and 31.9 (q, $J_{\text{CH}} = 127$ Hz, OCMe_3), 16.5 (dt, $J_{\text{CH}} = 125$ Hz, $J_{\text{CP}} = 19.8$ Hz, PCH_2CH_3), 8.5 ppm (q, $J_{\text{CH}} = 125$ Hz, PCH_2CH_3); $^{31}\text{P}\{^1\text{H}\}$ NMR (toluene- d_8 , 253 K) major isomer 31.3 ppm ($J_{\text{PW}} = 305$ Hz); minor isomer 29.3 ppm ($J_{\text{PW}} = 298$ Hz); major isomer/minor isomer ≈ 6 .

Preparation of $\text{W}(\text{O})(\text{CHCMe}_3)(\text{OCMe}_3)_2(\text{PMe}_2\text{Ph})$. This complex was prepared in a manner analogous to the preceding two from LiOCMe_3 (0.52 g, 6.5 mmol) in 20 mL of ether and $\text{W}(\text{O})(\text{CHCMe}_3)\text{Cl}_2(\text{PMe}_2\text{Ph})_2$ (2.0 g, 3.24 mmol) in 30 mL of ether at room temperature. The product is a thermally sensitive yellow oil.

^1H NMR (toluene- d_8 , 248 K) major isomer 9.77 (br s, 1, $J_{\text{HW}} = 9.8$ Hz, CHCMe_3), 6.99–7.44 (m, 5, PPh), 1.47 (s, 9, OCMe_3), 1.45 (s, 9, OCMe_3), 1.29 (d, 6, $^2J_{\text{HP}} = 13$ Hz, PMe_2), 1.24 ppm (s, 9, CHCMe_3). The minor isomer has its H_α resonance at ppm 10.64. ^{13}C NMR (toluene- d_8 , 223 K, gated proton decoupled) major isomer 269 (dd, $J_{\text{CH}} = 119$ Hz, $^2J_{\text{CP}} = 7.8$ Hz, $J_{\text{CW}} = 186$ Hz, CHCMe_3), 124–135 (m, PPh), 77.2 (s, OCMe_3), 74.9 (s, OCMe_3), 42.4 (s, CHCMe_3), 33.5 (q, $J_{\text{CH}} = 125$ Hz, CHCMe_3), 32.1 (q, $J_{\text{CH}} = 123$ Hz, OCMe_3), 14.9 (dq, $J_{\text{CH}} = 131$ Hz, $J_{\text{CP}} = 39.1$ Hz, PMe), 13.8 ppm (dq, $J_{\text{CH}} = 131$ Hz, $J_{\text{CP}} = 41.0$ Hz, PMe). The minor isomer has its C_α resonance at ppm 267 ($^2J_{\text{CP}} = 9.8$ Hz). $^{31}\text{P}\{^1\text{H}\}$ NMR (toluene- d_8 , 223 K) major isomer 7.2 ppm ($J_{\text{PW}} = 300$ Hz); minor isomer 8.1 ppm ($J_{\text{PW}} = 298$ Hz); major isomer/minor isomer ≈ 6 ; IR (Nujol) 949 cm^{-1} (s, br, $\nu_{\text{W-O}}$).

Preparation of $[\text{W}(\text{O})(\text{CHCMe}_3)(\text{OCMe}_3)_2]$. Anhydrous NET_4Cl (1.35 g, 8.12 mmol) was added to a solution of TaNP_2Cl_3 (1.75 g, 4.06 mmol) in 40 mL of CH_2Cl_2 . The orange-yellow solution immediately turned red. $\text{W}(\text{O})(\text{OCMe}_3)_4$ (2.0 g, 4.06 mmol) was added and the color lightened to orange in 0.5 h. The

solvent was removed in vacuo, leaving an orange-tan solid. This solid was washed five times with 20 mL of pentane. The pentane extracts were combined and filtered. The pentane was removed in vacuo, leaving 1.12 g (67%) of $[\text{W}(\text{O})(\text{CHCMe}_3)(\text{OCMe}_3)_2]_2$ as an orange oil. The pentane-insoluble tan solid had a ^1H NMR spectrum in CH_2Cl_2 consistent with $[\text{Ta}(\text{OCMe}_3)_2\text{Cl}_4]^-[\text{NEt}_4]^+$ [3.37 (q, 4, $^3J_{\text{HH}} = 7$ Hz, NCH_2CH_3), 1.47 (t, 6, $^3J_{\text{HH}} = 7$ Hz, NCH_2CH_3), 1.47 ppm (s, 9, OCMe_3)].

^1H NMR (C_6D_6) 10.68 (s, 1, $J_{\text{HW}} = 12.1$ Hz, CHCMe_3), 1.45 (s, 9, OCMe_3), 1.41 (s, 9, OCMe_3), 1.16 ppm (s, 9, CHCMe_3); ^{13}C NMR (toluene- d_8 , 268 K, gated proton decoupled) 290 (d, $J_{\text{CH}} = 135$ Hz, $J_{\text{CW}} = 156$ Hz, CHCMe_3), 91.9 (s, OCMe_3), 90.4 (s, OCMe_3), 42.5 (s, CHCMe_3), 32.6 (q, $J_{\text{CH}} = 123$ Hz, CHCMe_3), 29.7 and 29.5 ppm (q, $J_{\text{CH}} = 123$ Hz, OCMe_3); IR (Nujol) 940 cm^{-1} (s, br, $\nu_{\text{W-O}}$) mol wt (cryoscopy in cyclohexane) calcd, 834; found, 640.

Acknowledgment. We thank the National Science Foundation for supporting this research (CHE 79 05307). R.R.S. thanks the Camille and Henry Dreyfus Foundation for a Teacher-Scholar Award (1978).

Registry No. $\text{W}(\text{O})(\text{OCMe}_3)_4$, 58832-09-0; $\text{W}(\text{O})(\text{CHCMe}_3)\text{Cl}_2(\text{PMe}_2)_2$, 76603-92-4; $\text{W}(\text{O})(\text{CHCMe}_3)\text{Cl}_2(\text{PET}_3)_2$, 74666-77-6; $\text{W}(\text{O})(\text{CHCMe}_3)\text{Cl}_2(\text{PMe}_2\text{Ph})_2$, 79329-25-2; $\text{W}(\text{O})(\text{CHCMe}_3)\text{Br}_2(\text{PET}_3)_2$, 79329-26-3; $\text{W}(\text{O})(\text{CHCMe}_3)\text{Cl}_2(\text{PET}_3)$, 74658-29-0; $\text{W}(\text{O})(\text{CHCMe}_3)\text{Cl}_2(\text{PMe}_3)(\text{PhCN})$, 79357-00-9; $\text{W}(\text{O})(\text{CHCMe}_3)\text{Cl}_2(\text{PMe}_3)(\text{THF})$, 79329-27-4; $\text{W}(\text{O})(\text{CHCMe}_3)\text{Cl}_2(\text{tmeda})$, 79329-28-5; $[\text{W}(\text{O})(\text{CHCMe}_3)\text{Cl}(\text{PET}_3)_2]^+(\text{AlCl}_4^-)$, 79357-56-5; $[\text{W}(\text{O})(\text{CHCMe}_3)(\text{PET}_3)_2]^{2+}(\text{AlCl}_4^-)_2$, 79357-52-1; $[\text{W}(\text{O})(\text{CHCMe}_3)(\text{Me})(\text{PET}_3)_2]^+(\text{AlMe}_2\text{Cl}_2^-)$, 79357-54-3; $\text{W}(\text{O})(\text{CHCMe}_3)\text{MeCl}(\text{tmeda})$, 79329-29-6; $[\text{W}(\text{O})(\text{CHCMe}_3)(\text{AlMe}_2)(\text{PET}_3)_2]^+(\text{AlMe}_2\text{Cl}_2^-)$, 79329-32-1; $[\text{W}(\text{O})(\text{CHCMe}_3)\text{Cl}(\text{PET}_3)]^+(\text{AlCl}_4^-)$, 79357-58-7; $\text{W}(\text{O})(\text{CHCMe}_3)\text{Cl}(\text{F})(\text{PET}_3)_2$, 79329-33-2; $\text{W}(\text{O})(\text{CHCMe}_3)(\text{S}_2\text{CNMe}_2)_2$, 79329-34-3; $\text{W}(\text{O})(\text{CHCMe}_3)(\text{OCMe}_3)_2(\text{PMe}_3)$, 79329-35-4; $\text{W}(\text{O})(\text{CHCMe}_3)(\text{OCMe}_3)_2(\text{PET}_3)$, 79329-36-5; $\text{W}(\text{O})(\text{CHCMe}_3)(\text{OCMe}_3)_2(\text{PMe}_2\text{Ph})$, 79329-37-6; $[\text{W}(\text{O})(\text{CHCMe}_3)(\text{OCMe}_3)_2]_2$, 79329-38-7; $\text{W}(\text{O})\text{Cl}_4$, 13520-78-0; $\text{Ta}(\text{CHCMe}_3)\text{Cl}_3(\text{PMe}_3)_2$, 70083-62-4; $\text{Ta}(\text{CHCMe}_3)\text{Cl}_3(\text{PET}_3)_2$, 77126-35-3; $[\text{Ta}(\text{OCMe}_3)_4\text{Cl}_2]$, 79357-59-8.

Electrochemical Oxidation–Reduction of Organometallic Complexes. Effect of the Oxidation State on the Pathways for Reductive Elimination of Dialkyliron Complexes

W. Lau, J. C. Huffman, and J. K. Kochi*

Department of Chemistry, Indiana University, Bloomington, Indiana 47405

Received July 31, 1981

A series of octahedral dialkylbis(α,α' -bipyridine)iron(II) complexes A are synthesized and shown to exist in the cis configuration, both in the crystal and in solution. Transient electrochemical techniques are used to identify two other oxidation states, viz., the dialkyliron(III) cation B and the dialkyliron(IV) dication C. The $\text{A} \rightleftharpoons \text{B}$ couple is electrochemically reversible, and crystalline dialkyliron(III) salts of B can be isolated and their anisotropic ESR spectra resolved into the three principal elements of the \mathbf{g} tensor (showing rhombic symmetry). The $\text{B} \rightleftharpoons \text{C}$ couple is electrochemically irreversible, but cyclic voltammetric studies indicate that C is formed by a rate-limiting oxidation. Both B and C retain the cis configuration of the alkyl ligands in solution. Each of the dialkyliron species undergoes a characteristic pathway for reductive elimination. Thus the disproportionation of the alkyl ligands to alkane and alkene in A derives via β -elimination from a coordinatively unsaturated intermediate. Homolytic fragmentation of B leads to products arising from the cage reactions of alkyl radicals. On the other hand, the concerted loss of both alkyl ligands in C leads to coupled dialkyls in excellent yields. The comparative behavior of the isomeric dialkyliron species A, B, and C is discussed in terms of the driving force for reductive elimination. The general principles are illustrated briefly in the comparative carbonylation of A and B with CO.

Introduction

Owing to the importance of organometallic intermediates in a variety of catalytic reactions,¹⁻⁴ it is necessary to

identify those factors which determine how the carbon-metal bond can be selectively cleaved. Organometals are

(1) Masters, C. "Homogeneous Transition-metal Catalysis"; Chapman and Hall: London, 1981.

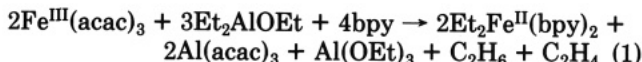
(2) Parshall, G. W. "Homogeneous Catalysis. The Applications and Chemistry of Catalysis by Soluble Transition Metal Complexes"; Wiley: New York, 1980.

recognized as excellent electron donors by virtue of the powerful effect exerted by alkyl groups as σ -donor ligands.⁵⁻⁷ Coupled with the ubiquity of oxidation-reduction processes in catalytic cycles, such as the many types of oxidative additions and reductive eliminations,⁸ it is reasonable to inquire whether changes in the oxidation state of an organometal affects its reactivity and mode of reaction.⁹

In a preliminary study,¹⁰ we showed that otherwise stable organometallic complexes can be induced to undergo facile reductive elimination when subjected to oxidation. At that time, the use of chemical oxidants did not allow a rigorous identification of the organometallic intermediates actually involved in the reductive elimination. The development of transient electrochemical techniques¹¹ now permits us to probe the oxidation-reduction properties of organometals and to identify the various pathways for reductive elimination.¹² In this study, we have focused our attention on the redox behavior of the series of dialkylbis(α,α' -bipyridine)iron(II) complexes in which the presence of a pair of alkyl ligands can be exploited in mechanistic studies of reductive elimination.

Results

The original synthesis of diethylbis(α,α' -bipyridine)iron(II) A by Yamamoto and co-workers involves the reductive alkylation of tris(acetylacetonato)iron(III) with excess diethylaluminum ethoxide in the presence of α,α' -bipyridine according to the presumed stoichiometry in eq 1.¹³ We also prepared the methyl and *n*-propyl ana-



logues by a similar procedure starting with the commercially available trimethyl- and tri-*n*-propylalanes, respectively. Unfortunately, the application of this synthetic method to other alkyl derivatives is severely limited by the availability of the corresponding organoaluminum reagent.

I. Synthesis and Structure of Dialkylbis(bipyridine)iron(II) Complexes. The direct alkylation of the readily available dichlorobis(α,α' -bipyridine)iron(II) represents a more direct and convenient route to A. For example, ethyllithium undergoes ready metathesis with

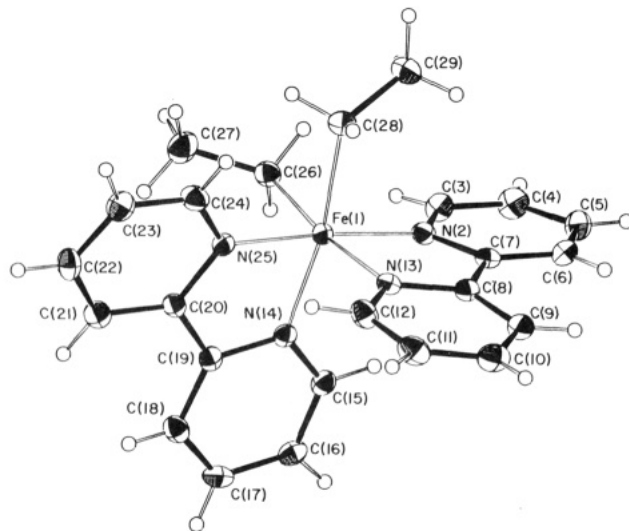
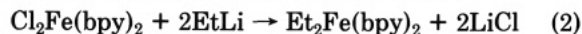
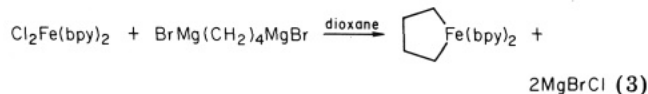


Figure 1. ORTEP drawing of the structure of diethylbis(α,α' -bipyridine)iron(II). Anisotropic thermal ellipsoids are drawn at the 50% probability level. Hydrogen atoms are portrayed at 0.5 Å².

$\text{Cl}_2\text{Fe}(\text{bpy})_2$ in toluene to afford the diethyliron(II) complex in high yields according to the stoichiometry



The course of alkylation is visually apparent by the dissolution of the insoluble, dark red $\text{Cl}_2\text{Fe}(\text{bpy})_2$ to the soluble, deep blue solution of A, even at -78°C . The insolubility of lithium chloride in hydrocarbon media enables the product to be separated easily and purified. Moreover, the accessibility of various alkyl lithium reagents allows this synthetic procedure to be widely applicable, particularly to *n*-alkyl derivatives. Alkylation in eq 2 may also be effected by various Grignard reagents (if it is carried out in the presence of 1,4-dioxane to precipitate the magnesium halide), as in the synthesis of the ferracyclopentane in eq 3. The secondary and tertiary alkyl



analogues such as the isopropyl and *tert*-butyl derivatives of A are thermally too unstable to isolate, since they decompose rapidly in solution, even at -20°C . Highly hindered alkyl ligands such as neopentyl effect metathesis very slowly, and the dialkyliron(II) complex cannot be obtained in pure form.¹⁴

In order to determine the molecular structure of these dialkyliron(II) complexes, particularly with regard to the disposition of the alkyl groups, we grew a single crystal of the diethyl derivative of A under carefully controlled conditions (see Experimental Section). The X-ray diffraction data were collected at -173°C to reduce thermal vibrations and permit the location and refinement of all hydrogen atoms. The quality of the crystal data is shown by the final residuals [$R(F) = 0.0408$ and $R_w(F) = 0.0419$] and a goodness of fit for the last cycle of 1.008. The relevant bond distances and bond angles in $\text{Et}_2\text{Fe}(\text{bpy})_2$ are included in Table I. The crystal structure in Figure 1 delineates the octahedral configuration about the iron center in A and clearly reveals the pair of ethyl ligands in

(14) Dialkylbis(bipyridine)iron(II) complexes undergo an accelerated decomposition in the presence of excess alkyl lithium and Grignard reagents. Consequently, the metathesis in eq 2 or 3 must occur readily; otherwise decomposition of A becomes competitive with its formation.

(3) Heck, R. F. "Organotransition Metal Chemistry"; Academic Press: New York, 1974.

(4) Collman, J. P.; Hegedus, L. S. "Principles and Applications of Organotransition Metal Chemistry"; University Science Books: Mill Valley, CA, 1980.

(5) Jonas, A. E.; Schweitzer, G. K.; Grimm, F. A.; Carlson, T. A. *J. Electron Spectrosc. Relat. Phenom.* **1972**, *1*, 29.

(6) (a) Evans, S.; Green, J. C.; Joachim, P. J.; Orchard, A. F.; Turner, D. W.; Maier, J. P. *J. Chem. Soc., Faraday Trans. 2*, **1972**, *68*, 905. (b) Boschi, R.; Lappert, M. F.; Pedley, J. B.; Schmidt, W.; Wilkins, B. T. *J. Organomet. Chem.* **1973**, *50*, 69.

(7) Fehlner, T. P.; Ulman, J.; Nugent, W. A.; Kochi, J. K. *Inorg. Chem.* **1976**, *15*, 2544.

(8) Kochi, J. K. "Organometallic Mechanisms and Catalysis", Academic Press: New York, 1978.

(9) Cf. Daub, G. W. *Prog. Inorg. Chem.* **1977**, *22*, 409. Lalaev, V. V.; Belov, A. P. *Z. Obsch. Khim.* **1976**, *46*, 2753.

(10) Tsou, T. T.; Kochi, J. K. *J. Am. Chem. Soc.* **1978**, *100*, 1634.

(11) (a) Klingler, R. J.; Kochi, J. K. *J. Am. Chem. Soc.* **1980**, *102*, 4790.

(b) Klingler, R. J.; Kochi, J. K. *J. Phys. Chem.* **1981**, *85*, 1731.

(12) (a) Tamblyn, W. H.; Klingler, R. J.; Hwang, W. S.; Kochi, J. K. *J. Am. Chem. Soc.* **1981**, *103*, 3161. (b) Klingler, R. J.; Huffman, J. C.; Kochi, J. K. *Ibid.* **1980**, *102*, 208. (c) Klingler, R. J.; Kochi, J. K. *Inorg. Chem.* **1981**, *20*, 34. (d) Klingler, R. J.; Kochi, J. K. *J. Organomet. Chem.* **1980**, *202*, 49.

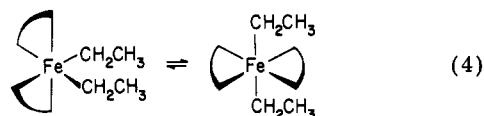
(13) Yamamoto, A.; Morifuji, K.; Ikeda, S.; Saito, T.; Uchida, Y.; Misono, A. *J. Am. Chem. Soc.* **1968**, *90*, 1878. Compare: Tamura, M.; Kochi, J. K. *Bull. Chem. Soc. Jpn.* **1971**, *44*, 3063.

Table I. Relevant Bond Distances (Å) and Bond Angles (Deg) in Et₂Fe(bpy)₂

A	B	dist	A	B	dist
Fe(1)	N(2)	1.937 (2)	C(6)	C(7)	1.397 (3)
Fe(1)	N(13)	1.985 (2)	C(7)	C(8)	1.456 (3)
Fe(1)	N(14)	1.976 (2)	C(8)	C(9)	1.395 (3)
Fe(1)	N(25)	1.943 (2)	C(9)	C(10)	1.376 (4)
Fe(1)	C(26)	2.068 (2)	C(10)	C(11)	1.391 (4)
Fe(1)	C(28)	2.063 (2)	C(11)	C(12)	1.367 (4)
N(2)	C(3)	1.369 (3)	C(15)	C(16)	1.379 (3)
N(2)	C(7)	1.372 (3)	C(16)	C(17)	1.383 (4)
N(13)	C(8)	1.359 (3)	C(17)	C(18)	1.379 (4)
N(13)	C(12)	1.362 (3)	C(18)	C(19)	1.396 (3)
N(14)	C(15)	1.348 (3)	C(19)	C(20)	1.451 (3)
N(14)	C(19)	1.371 (3)	C(20)	C(21)	1.392 (3)
N(25)	C(20)	1.371 (3)	C(21)	C(22)	1.376 (4)
N(25)	C(24)	1.362 (3)	C(22)	C(23)	1.390 (4)
C(3)	C(4)	1.364 (4)	C(23)	C(24)	1.368 (4)
C(4)	C(5)	1.389 (4)	C(26)	C(27)	1.516 (4)
C(5)	C(6)	1.374 (4)	C(28)	C(29)	1.521 (3)

A	B	C	angle	A	B	C	angle
N(2)	Fe(1)	N(13)	80.4 (1)	C(4)	C(5)	C(6)	118.1 (2)
N(2)	Fe(1)	N(14)	95.9 (1)	C(5)	C(6)	C(7)	120.0 (2)
N(2)	Fe(1)	N(25)	174.7 (1)	N(2)	C(7)	C(6)	122.3 (2)
N(2)	Fe(1)	C(26)	92.3 (1)	N(2)	C(7)	C(8)	113.6 (2)
N(2)	Fe(1)	C(28)	91.9 (1)	C(6)	C(7)	C(8)	124.1 (2)
N(13)	Fe(1)	N(14)	95.6 (1)	N(13)	C(8)	C(7)	112.8 (2)
N(13)	Fe(1)	N(25)	95.6 (1)	N(13)	C(8)	C(9)	122.6 (2)
N(13)	Fe(1)	C(26)	171.7 (1)	C(7)	C(8)	C(9)	124.5 (2)
N(13)	Fe(1)	C(28)	91.1 (1)	C(8)	C(9)	C(10)	119.2 (2)
N(14)	Fe(1)	N(25)	80.9 (1)	C(9)	C(10)	C(11)	118.7 (2)
N(14)	Fe(1)	C(26)	89.2 (1)	C(10)	C(11)	C(12)	119.5 (2)
N(14)	Fe(1)	C(28)	170.4 (1)	N(13)	C(12)	C(11)	123.3 (2)
N(25)	Fe(1)	C(26)	91.9 (1)	N(14)	C(15)	C(16)	123.6 (2)
N(25)	Fe(1)	C(28)	91.7 (1)	C(15)	C(16)	C(17)	119.3 (2)
C(26)	Fe(1)	C(28)	85.0 (1)	C(16)	C(17)	C(18)	118.6 (2)
Fe(1)	N(2)	C(3)	127.5 (2)	C(17)	C(18)	C(19)	119.7 (2)
Fe(1)	N(2)	C(7)	116.7 (2)	N(14)	C(19)	C(18)	121.9 (2)
C(3)	N(2)	C(7)	115.7 (2)	N(14)	C(19)	C(20)	113.3 (2)
Fe(1)	N(13)	C(8)	116.1 (2)	C(18)	C(19)	C(20)	124.8 (2)
Fe(1)	N(13)	C(12)	127.2 (2)	N(25)	C(20)	C(19)	113.6 (2)
C(8)	N(13)	C(12)	116.7 (2)	N(25)	C(20)	C(21)	122.9 (2)
Fe(1)	N(14)	C(15)	127.7 (2)	C(19)	C(20)	C(21)	123.5 (2)
Fe(1)	N(14)	C(19)	115.4 (2)	C(20)	C(21)	C(22)	119.7 (2)
C(15)	N(14)	C(19)	116.9 (2)	C(21)	C(22)	C(23)	117.8 (2)
Fe(1)	N(25)	C(20)	116.1 (2)	C(22)	C(23)	C(24)	120.1 (2)
Fe(1)	N(25)	C(24)	128.3 (2)	N(25)	C(24)	C(23)	123.6 (2)
C(20)	N(25)	C(24)	115.6 (2)	Fe(1)	C(26)	C(27)	119.6 (2)
N(2)	C(3)	C(4)	123.8 (2)	Fe(1)	C(28)	C(29)	119.6 (2)
C(3)	C(4)	C(5)	119.9 (2)				

a cis relationship. The latter differs from the earlier suggestion by Yamamoto and co-workers that A is a *trans*-diethylbis(bipyridine)iron(II) complex.¹⁵ However, it is possible for Et₂Fe(bpy)₂ in solution to be in dynamic equilibrium between cis and trans isomers, i.e., eq 4.



Fortunately, these isomers can be readily differentiated on the basis of the prochirality of the methylene protons in the ethyl ligands, which are enantiotopic in the *trans* isomer and diastereotopic in the *cis* isomer. The ¹H NMR spectrum of the ethyl ligands of A in benzene solution consists of a well-resolved ABX₃ pattern (see Experimental Section), as required by the *cis* configuration. The absence of significant temperature effects on the NMR spectrum indicates that Et₂Fe(bpy)₂ is more or less locked in the *cis* configuration in solution, as it is in the crystal.

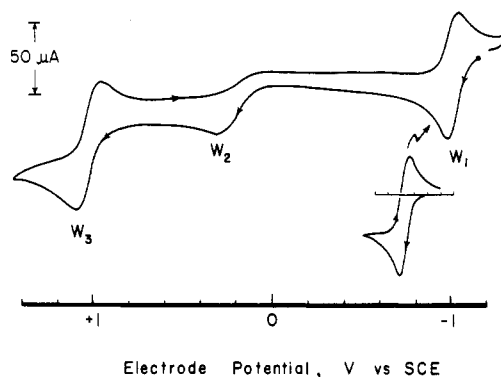
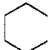


Figure 2. Single scan cyclic voltammogram of 1×10^{-3} M Me₂Fe(bpy)₂ at 100 mV s^{-1} in acetonitrile solution containing 0.1 M tetraethylammonium perchlorate at 25°C . The initial positive scan commences at $-1.5 \text{ V vs. NaCl SCE}$. The inset shows the reversible character of the wave marked W₁ at a scan rate of 10 mV s^{-1} .

II. Electrochemistry of Dialkylbis(bipyridine)-iron(II) Complexes. The Formation of Dialkyliron-(III) Cations and Dialkyliron(IV) Dications. The redox behavior of the dialkyliron(II) complexes A was

(15) Yamamoto, A.; Morifujii, K.; Ikeda, S.; Saito, T.; Uchida, Y.; Misono, A. *J. Am. Chem. Soc.* 1965, 87, 4652.

Table II. Cyclic Voltammetry of Dialkyliron(II) Complexes A^a

R ₂ Fe(bpy) ₂	solvent	W ₁ ^b E ⁰ (Δ, mV) ^c	W ₂ ^b E _p ^a	W ₃ ^b E ⁰
Me	CH ₃ CN	-1.02 (77)	+0.30	+1.03
Et	CH ₃ CN	-1.03 (65)	+0.20	+1.03
Et	acetone	-1.04 (93)	+0.11	d
<i>n</i> -Pr	CH ₃ CN	-1.05 (60)	+0.17	+1.05
<i>n</i> -Bu	acetone	-1.01 (90)	+0.22	d
	CH ₃ CN	-1.03 (70)	+0.20	+1.03

^a All potentials in volts relative to saturated NaCl SCE.

^b In relation to the waves labeled in Figure 2. ^c Separation of the anodic and cathodic peaks at a scan rate of 50 mV s⁻¹. ^d Solvent oxidation prevented the observation of the third wave.

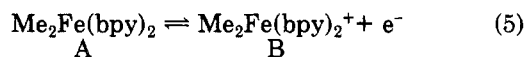
initially examined by electrochemical methods, using tetraethylammonium perchlorate (TEAP) as the supporting electrolyte.

A. Cyclic Voltammetry of Dialkyliron(II) Complexes. The single sweep cyclic voltammogram (CV) of Me₂Fe(bpy)₂ in Figure 2 shows the existence of three distinct oxidative processes on a positive potential scan commencing at -1.5 V vs. saturated NaCl SCE. The first wave (W₁), which appears to be a reversible oxidation with E⁰ = -1.03 V, is followed by an irreversible wave (W₂) with the anodic peak potential E_p^a = 0.20 V. The third wave (W₃) corresponds to reversible oxidation of Fe(bpy)₃²⁺.

The cyclic voltammograms of all the dialkyliron(II) complexes listed in Table II show three similar oxidative processes in common with the dimethyl analogue A, described above. Although these organometals undergo decomposition in acetonitrile solution, the process is sufficiently slow to enable meaningful CV measurements to be made. The cyclic voltammograms in acetone and in tetrahydrofuran (THF) were similar to those obtained in CH₃CN, but the waves were much broader in THF owing to the high ohmic resistance.

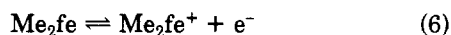
The reduction of the dialkyliron(II) complexes A was also examined by an initial negative potential scan. However, no cathodic process was observed in any of the derivatives prior to the reduction limit of the solvent (i.e., -1.9 V for CH₃CN and -1.4 V for acetone).

B. Controlled Potential Oxidations of Dialkyliron Species. Since the dimethyliron(II) analogue of A was the most stable in CH₃CN, it was used in further coulometric studies. The controlled potential oxidation of Me₂Fe(bpy)₂ at -0.35 V (which represents a potential between waves W₁ and W₂ in Figure 2) liberated one electron per iron. The electrolysis was accompanied by a marked change from the deep blue color of A to a dark green solution. The color change was reversible. Thus the controlled potential reduction of the green solution at -1.35 V regenerated the original deep blue solution, and coulometry showed that it required one electron per iron, i.e., eq 5.



Several tests were performed to elucidate the possibility of a secondary chemical reaction initiated by the oxidation, i.e., an EC mechanism of the type shown in Scheme I,

Scheme I



where fe = Fe(bpy)₂. If the follow-up reaction in eq 7 takes place on the time scale of the CV experiment, a depen-

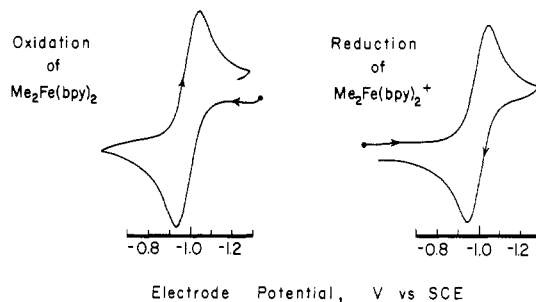


Figure 3. Cyclic voltammograms at 100 mV s⁻¹ showing the reversible oxidation-reduction of 5 × 10⁻³ M dialkyliron(II) and dialkyliron(III) in CH₃CN containing 0.1 M TEAP at 25 °C: left, initial positive scan for the oxidation of Me₂Fe(bpy)₂; right, initial negative scan for the reduction of Me₂Fe(bpy)₂⁺.

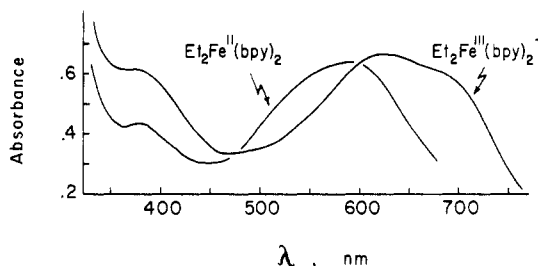


Figure 4. Visible absorption spectrum of 1 × 10⁻³ M Et₂Fe(bpy)₂ and ~3 × 10⁻³ M Et₂Fe(bpy)₂⁺ClO₄⁻ in tetrahydrofuran solutions.

dence of E⁰ on the sweep rate *v* should be observed.¹⁶ A 1 × 10⁻² M solution of A was used in the experiment, and the cyclic voltammogram of the first wave (W₁) was monitored between -1.35 and -0.35 V at sweep rates increasing incrementally from *v* = 20 to 800 mV s⁻¹. No change in E⁰ was noted or in an equivalent CV carried out in more dilute solutions. Chronoamperometry was further employed in a double potential step experiment conducted at the millisecond time scale, by utilizing a transient recorder and a sine wave generator for triggering between -1.35 and -0.35 V. It also indicated the oxidative process in eq 5 to be an uncomplicated electron-transfer process (see Experimental Section). The reversible one-electron reorganization in eq 5 must occur with minimal structural reorganization of the skeletal framework, since the cyclic voltammograms of the neutral iron(II) complex A and the iron(III) cation B are the same, as shown by the initial positive potential scan in Figure 3 (left) and the initial negative scan in Figure 3 (right), respectively.¹⁷

The reversible one-electron oxidation of the iron(II) complex in eq 5 is characteristic of all the alkyl derivatives. Thus, the controlled potential oxidation at -0.35 V of the ethyl and *n*-propyl analogues of A as well as the ferracyclopentane cleanly liberated one electron per iron to generate the corresponding iron(III) cation B. The electronic absorption spectrum of the diethyliron(III) cation B in Figure 4 shows the visible band to be red-shifted relative to that in the iron(II) analogue A, previously reported by Yamamoto and co-workers.¹³

The further oxidation of the cationic iron(III) species B is represented by the irreversible CV wave W₂ in Figure 2. Thus, the anodic oxidation of the green solution of the dimethyliron(III) cation Me₂Fe(bpy)₂⁺ at 0.8 V (which

(16) Nicholson, R. S.; Shain, I. *Anal. Chem.* 1964, 36, 706.

(17) The time scale for the transient electrochemical experiments is approximately seconds and if any reversible changes were to occur, they must be faster than this interval.¹⁸

(18) Bard, A. J.; Faulkner, L. R. "Electrochemical Methods"; Wiley: New York, 1980. MacDonald, D. D. "Transient Techniques in Electrochemistry"; Plenum Press: New York, 1977.

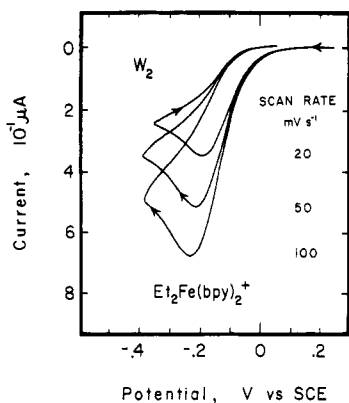
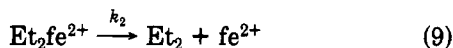
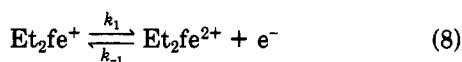


Figure 5. The initial positive scan cyclic voltammogram of $\sim 3 \times 10^{-3}$ M $\text{Et}_2\text{Fe}(\text{bpy})_2^+\text{ClO}_4^-$ in acetone containing 0.1 M TEAP at a platinum microelectrode using various sweep rates at 0 °C. Electrode potentials are in volts vs. saturated SCE.

represents a potential between waves W_2 and W_3) liberated one electron per iron and was accompanied by the precipitation of a brick-red solid and concomitant evolution of a gas (ethane). Similarly, the anodic oxidation of the deep blue solution of the neutral iron(II) complex $\text{Me}_2\text{Fe}(\text{bpy})_2$ at the same potential of 0.8 V gave up two electrons per iron (by coulometric determination) and produced the same mixture of red solid, gas, and the final pale pink solution. Since the one-electron oxidation of the dialkyliron(III) cation is clearly irreversible, we applied transient electrochemical techniques to probe the nature of this process.

The initial positive scan cyclic voltammograms of all the dialkyliron(III) cations are characterized by an anodic wave showing a well-defined current maximum, but no coupled cathodic wave on the reverse scan even at sweep rates up to 10^3 mV s^{-1} and temperatures as low as -78 °C. The details of the sweep dependence of the anodic wave are shown in Figure 5 for the diethyliron(III) cation B, as a representative of this system. A closer inspection of the cyclic voltammograms reveals that the current in the foot of the anodic wave is singularly independent of the sweep rate. Such a behavior, originally noted by Reinmuth¹⁹ and detailed with a variety of other organometallic species,^{11,12} was the first indication that electron transfer from $\text{Et}_2\text{Fe}(\text{bpy})_2^+$ is electrochemically unidirectional, i.e., totally irreversible. The more rigorous criteria required to establish total irreversibility are detailed in the Experimental Section. Suffice it to mention here that the absence of the reverse electron-transfer step has been shown to derive from the rapid decomposition of the intermediate, i.e., the diethyliron(IV) dication C in Scheme II for which $k_2 \gg k_{-1}$.²⁰ Indeed independent measurements employing double potential step chronoamperometry have established the lifetime of such species to be less than 1 ms.^{11,21}

Scheme II



(19) Reinmuth, W. H. *Anal. Chem.* 1960, 32, 1891.

(20) (a) Although iron(IV) complexes are rare, the presence of such donor ligands as α,α' -bipyridine and alkyl groups confers stability to this high oxidation state, discussed generally in ref 8, chapter 15. As an example, tetrakis(1-norbornyl)iron is an isolable, stable organoiron(IV) complex. [Bowers, B. K.; Tennent, H. G. *J. Am. Chem. Soc.* 1972, 94, 2512.] (b) Alternatively, there is no bound state corresponding to the dication, and electron transfer is a dissociative process. In view of our earlier studies (see especially ref 12a), we consider this an unlikely possibility.

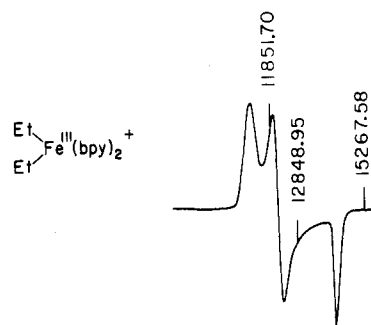


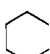
Figure 6. ESR spectrum of diethylbis(bipyridine)iron(III) perchlorate (0.05 M) in THF solution frozen at -180 °C. NMR field markers are in kHz.

Table III. Anisotropic ESR Parameters for Dialkyliron(III) Cations B^a

$\text{R}_2\text{Fe}(\text{bpy})_2^+\text{ClO}_4^-$	g_x	g_y	g_z
Me	2.4608	2.2817	1.9370
Et	2.4805	2.2739	1.9459
<i>n</i> -Pr	2.4825	2.2698	1.9343

^a Spectra recorded in THF frozen at -180 ± 10 °C.

Table IV. Hydrocarbon Products of the Thermal Decomposition of Dialkyliron(II) Complexes A^a

$\text{R}_2\text{Fe}(\text{bpy})_2$ R (μmol)	solvent	alkane, μmol (%) ^b	alkene, μmol (%) ^b
Et (50)	benzene	52 (104)	34 (68)
Et (50)	THF	52 (104)	37 (74)
<i>n</i> -Pr (50)	THF	60 (120)	23 (46)
<i>n</i> -Bu (12.7)	benzene	13 (102)	8 (63)
 (32.1)	THF	15 (47) ^c	14 (44) ^d

^a Duplicate runs in 1 mL solution at 50 °C. ^b Based on mol hydrocarbon per mol of dialkyliron(II). ^c Butane.

^d 1-Butene.

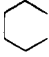
C. Isolation and ESR Spectra of Dialkylbis(bipyridine)iron(III) Cations. The controlled-potential oxidation of the dialkyliron(II) complexes A at -0.4 V always resulted in the characteristic dark green solution of the iron(III) cation B. These iron(III) cations can be isolated as crystalline perchlorate salts if the anodic oxidation is carried out in THF solution with 0.2 M TBAP and the product precipitated with ether. After repeated attempts, we were unsuccessful in growing single crystals of any derivative of B which were suitable for X-ray crystallography.

The esr spectrum of the diethyliron(III) cation B in THF frozen at -180 °C is shown in Figure 6. The anisotropic g tensors, g_x , g_y , and g_z , are well-resolved in this non-oriented, low-spin iron(III) system with orthorhombic symmetry.²² The latter is consistent with the cis configuration of II, already deduced from the cyclic voltammetry experiments (vide supra). The g tensors of the related dimethyl- and di-*n*-propyl analogues are included in Table III for comparison. No nitrogen hyperfine splittings arising from the bipyridine ligands were resolved upon temperature variation. The lines gradually broadened as the

(21) The facile reductive elimination of organometal cations is described in ref 11 and 12. See also: Wong, C. L.; Kochi, J. K. *J. Am. Chem. Soc.* 1979, 101, 5593. Chen, J. Y.; Gardner, H. C.; Kochi, J. K. *Ibid.* 1976, 98, 6150. Chen, J. Y.; Kochi, J. K. *Ibid.* 1977, 99, 1450. Gardner, H. C.; Kochi, J. K. *Ibid.* 1975, 97, 1855.

(22) The details of the analysis of the esr spectra will be published separately. Chen, K. S., unpublished results.

Table V. Hydrocarbon Products from the Thermal Decomposition of Dialkyliron(III) Cations B^a

R ₂ Fe-(bpy) ₂ ⁺ ClO ₄ ⁻ R (μmol)	solvent (mL)	hydrocarbons, μmol		
		alkane	alkene	dialkyl
Me	23.9	THF (6)	15	12
Et	25	THF (25)	17	3.5
	25	THF (5)	14	3.5
	15	acetone (4)	10	2.5
n-Pr	12	THF (2)	7.1	0.8
Et	26	} THF (7)	b	b
n-Pr	26			2.7, ^c 11 ^d
	9.2	THF (14)	0.8 ^e	0.3 ^f
	9.2	THF (4) ^h	0.8 ^e	0.3 ^f
	9.2	THF (4)	1.1 ^e	0.2 ^f

^a At 30 °C, generated electrochemically at -0.35 V.

^b C₂H₄, C₂H₆, C₃H₆, C₃H₈, and n-C₄H₁₀ present but not analyzed. ^c Pentane. ^d Hexane. ^e Butane. ^f 1-Butene.

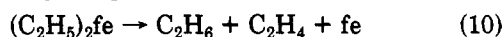
^g Cyclobutane. ^h Contains 400 μmol of bpy.

temperature was increased to -140 °C. However, the line broadening was completely reversible, the spectrum being unobservable at ~-70 °C owing to a short T₂ relaxation time in these dialkyliron(III) cations.²³

III. Reductive Eliminations of the Dialkylbis(bipyridine) Derivatives of Fe(II), Fe(III), and Fe(IV). The electrochemical studies thus clearly reveal the availability of three discrete dialkyliron species A, B, and C, which differ only in the oxidation state of the iron center. Let us now describe how each of these species undergoes reductive elimination.

Dialkyliron(II) Complex A. The thermal decomposition of diethylbis(bipyridine)iron(II) was examined by Yamamoto et al. in an earlier study.²⁴ Following their results, we also observe the reductive elimination of ethane and ethylene at 50 °C in either benzene or THF solution. A careful search indicated no butane (<0.1%).

Although the thermolysis can be generally described by the stoichiometry in eq 10, the reductive elimination is not



quite so straightforward. Thus the results in Table IV show that the alkane is always formed in a slight, but definite excess relative to the alkene. The hydrogen discrepancy is pronounced in the decomposition of the ferrocyclopentane A, in which 1-butene (the direct product of reductive elimination)²⁵ is supplemented by substantial amounts of butane derived from a reduction. If the extra hydrogens came from the solvent, it is not clear why the yield of alkanes in THF is not greater than that in benzene, despite its greater hydrogen donor properties. Furthermore, similar results have been observed in the decomposition of Et₂Fe(bpy)₂ in the solid state.²⁴

The decomposition of dialkylbis(bipyridine)iron(II) complexes produces an insoluble dark red precipitate which has been ascribed to a polymeric bis(bipyridine)iron(0) species,¹⁵ designated as fe for [Fe(bpy)₂]_x in eq 10.

(23) Cf. (a) Prins, R.; Kortbeek, A. G. T. G. *J. Organomet. Chem.* 1971, 33, C33. (b) Horsfield, A.; Wassermann, A. *J. Chem. Soc., Dalton Trans.* 1972, 187. (c) Merrithew, P. B.; Lo, C. C.; Modestino, A. J. *Inorg. Chem.* 1975, 14, 242. (d) Reiff, W. M.; DeSimone, R. E. *Inorg. Chem.* 1973, 12, 1793.

(24) Yamamoto, T.; Yamamoto, A.; Ikeda, S. *Bull. Chem. Soc. Jpn.* 1972, 45, 1104, 1111.

(25) Compare the decomposition of other metallacyclopentanes: (a) McDermott, J. X.; White, J. F.; Whitesides, G. M. *J. Am. Chem. Soc.* 1976, 98, 6521. (b) McDermott, J. X.; Wilson, M. E.; Whitesides, G. M. *Ibid.* 1976, 98, 6529. (c) Young, G. B.; Whitesides, G. M. *Ibid.* 1978, 100, 5808. (d) Grubbs, R. H.; Miyashita, A.; Liu, M.; Burk, P. *Ibid.* 1978, 100, 2418.

Table VI. Cage Disproportionation and Combination of Ethyl Radicals Generated in the Photolysis of Azoethane^a

solvent	additive	hydrocarbons, μmol			yield, %
		C ₂ H ₄	C ₂ H ₆	C ₄ H ₁₀	
THF		3.1	22	24	73
THF		3.2	22	24	74
THF	styrene ^b	3.9	4.7	26	60
THF	styrene ^c	3.7	4.1	25	58
toluene		4.8	22	28	83
toluene		4.6	21	28	81

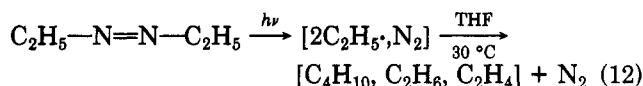
^a In 10-mL solution of 5 × 10⁻³ M EtN=NEt irradiated with a medium-pressure Hg lamp through a CuSO₄ filter at 30 °C. ^b 2 mol %. ^c 5 mol %.

In the presence of additional α,α'-bipyridine, the known tris(bipyridine)iron(0) is formed.²⁶

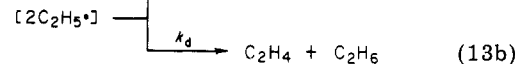
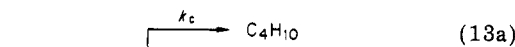
Dialkyliron(III) Cation B. The thermal decomposition of the dialkyliron(III) cation differs from that of the neutral dialkyliron(II) counterpart A in two ways. First, B is significantly less stable in solution, having a half-life of only ~30 min at 30 °C, whereas A is stable for days at this temperature. Second, the organic products of decomposition of R₂Fe(bpy)₂⁺ in Table V consist of a mixture of dialkyl (R₂) and alkane (RH), with smaller amounts of alkene (R-H). For example, the diethyliron(III) cation affords butane (45%), ethane (48%), and ethylene (8%) in THF solution.



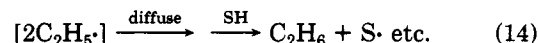
This product composition bears close resemblance to that expected from the cage reaction between a pair of ethyl radicals.²⁷ In order to simulate the latter, we photolyzed a solution of azoethane under the same reaction conditions, i.e.,²⁸ eq 12. Indeed the yields of butane, ethane, and



ethylene in Table VI compare remarkably well with those obtained from the decomposition of Et₂Fe(bpy)₂⁺ presented in Table V. Accordingly, the ratio of butane to ethylene (C₄H₁₀/C₂H₄ ≈ 6) is determined by the relative rates of combination and disproportionation (k_c/k_d = 6.5) of ethyl radical,²⁹ i.e., eq 13. The extra ethane (i.e., total



ethane minus ethylene) derives by hydrogen atom abstraction from the solvent, subsequent to diffusion from the cage



The essential correctness of the formulation in eq 13 and 14 is supported by three independent types of scavenging experiments involving styrene, deuteriated acetone, and nitrosodurene to trap the cage-escaped ethyl radicals. (a)

(26) Herzog, S.; Präkel, H. *Z. Chem.* 1965, 5, 469. Hall, F. S.; Reynolds, W. L. *Inorg. Chem.* 1966, 5, 931.

(27) Stefani, A. P. *J. Am. Chem. Soc.* 1968, 90, 1694. Stefani, A. P.; Thrower, G. F.; Jordan, C. F. *J. Phys. Chem.* 1969, 73, 1257.

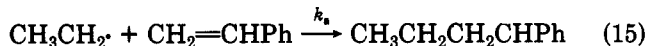
(28) Kodama, S.; Fujita, S.; Takeishi, J.; Toyama, O. *Bull. Chem. Soc. Jpn.* 1966, 39, 1009. Dixon, P. S.; Stefani, A. P.; Szwarc, M. *J. Am. Chem. Soc.* 1963, 85, 2551.

(29) Gibian, M. J.; Corley, R. C. *Chem. Rev.* 1973, 73, 441.

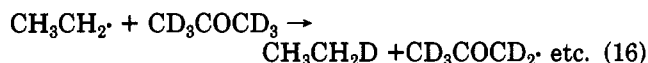


Figure 7. ESR spectrum of the spin adduct of ethyl radical and nitrosodurene obtained during the decomposition of 0.02 M $\text{Et}_2\text{Fe}(\text{bpy})_2^+\text{ClO}_4^-$ and 0.02 M nitrosodurene in THF at 30 °C.

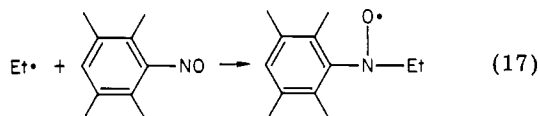
In the photolysis of azoethane, the presence of as little as 2% styrene is sufficient to completely quench the formation of the extra ethane through competition from the facile homolytic addition in eq 15.³⁰ As shown by the third



and fourth entries in Table VI, the yields of ethane and ethylene become equal, and they are in complete accord with the butane yields based on the rate constants for combination and disproportionation of ethyl radicals in eq 13, i.e., $\text{C}_4\text{H}_{10}/\text{C}_2\text{H}_4 = \text{C}_4\text{H}_{10}/\text{C}_2\text{H}_6 = k_c/k_d$. The use of 2–5 mol % of styrene as a radical trap in the thermal decomposition of $\text{Et}_2\text{Fe}(\text{bpy})_2^+$ induced a secondary reaction leading to the formation of excessive ethylene. Thus we resorted to two other traps, deuteriated acetone and nitrosodurene. (b) When the solvent is labeled with deuterium (e.g., perdeuterioacetone for SH in eq 14), the extent of cage escape is quantitatively measured by the fraction of the monodeuteriated ethane, i.e., eq 16. Mass



spectral analysis of the ethane liberated in the decomposition of $\text{Et}_2\text{Fe}(\text{bpy})_2^+$ in deuterioacetone indicated that 72% consists of $\text{C}_2\text{H}_5\text{D}$, by a comparison of the cracking pattern of an authentic mixture of C_2H_6 and $\text{C}_2\text{H}_5\text{D}$.³¹ Coupled with the product analysis, it is easy to conclude that all of the ethane in excess of ethylene acquired its extra hydrogen from the solvent (see Experimental Section). Neither the ethylene nor the butane showed any incorporation of deuterium. (c) The ethyl radicals formed in the thermal decomposition of $\text{Et}_2\text{Fe}(\text{bpy})_2^+$ can be identified as the spin adduct with nitrosodurene.³²



The ESR spectrum shown in Figure 7 is the same [$A_N = 13.6$ G, $A_{H_2} = 11.0$ G, ($g = 2.0058$)] as that of an authentic adduct obtained independently from the thermolysis of dipropionyl peroxide in the presence of nitrosodurene. Double integration of the ESR spectrum against a standard sample of DPPH indicated that the spin adduct accounted for 3–4% of all the ethyl groups liberated in the thermal decomposition of $\text{Et}_2\text{Fe}(\text{bpy})_2^+$, in basic accord with the formulation in eq 13 and 14.

Although most of the dialkyl (R_2) is derived by the cage combination of alkyl radicals as described in eq 13, a small amount must be also formed by the recombination of alkyl radicals which have suffered cage escape, as in eq 14.³³

(30) Cf. Ingold, K. U. *Free Radicals* 1973, 1, 91.

(31) It is unlikely that ethane- d_1 arises by a protonolysis mechanism, since the rate in acetone is similar to that in the aprotic THF (see Table VII).

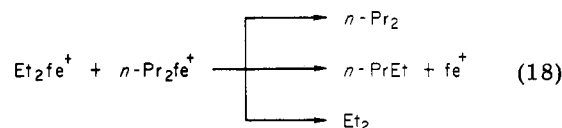
(32) Terabe, S.; Kuruma, K.; Konaka, R. *J. Chem. Soc., Perkin Trans. 2* 1973, 1252.

Table VII. First-Order Rate Constants (k_{obsd}) for Decomposition of Dialkyliron(III) Cations B^a

$\text{R}_2\text{Fe}(\text{bpy})_2^+\text{ClO}_4^-$	method ^b	solvent	$10^4 k_{\text{obsd}} \text{ s}^{-1}$
Me	polaro	THF	2.0
Et	polaro	THF	2.9
Et	spectro	THF	2.8
Et	spectro	THF ^c	2.7
Et	polaro	acetone	4.1
Et	polaro	acetone ^d	3.6
<i>n</i> -Pr	polaro	THF	3.6

^a In solutions containing 0.005 M dialkyliron(II) complex at 30 °C. ^b Polarographic analysis (see Experimental Section) or spectrophotometrically by following the visible band at 680 nm. Solution contains 0.2 M tetrabutylammonium perchlorate. ^c Contains 0.1 M α, α' -bipyridine.

The extent of the latter can be determined from the crossover when an equimolar mixture of $\text{Et}_2\text{Fe}(\text{bpy})_2^+$ and $n\text{-Pr}_2\text{Fe}(\text{bpy})_2^+$ is decomposed. The results in Table V (fourth entry) show that pentane is formed in about 5% yields, in addition to the homocoupled butane and hexane formed in major amounts, i.e., eq 18. Control experiments



demonstrate that the cross-coupled pentane did not arise via a prior exchange of ethyl and propyl ligands between the two cations.³⁴ Indeed the observation of the cross-coupling of alkyl ligands provides further support for the homolytic decomposition of dialkyliron(III) cations.

The rates of thermal decomposition of the dialkyliron(III) cations B follow clean first-order kinetics for more than 3 half-lives in either THF or acetone solution.³⁵

$$-\text{d}[\text{R}_2\text{Fe}^+]/\text{dt} = k_{\text{obsd}}[\text{R}_2\text{Fe}^+] \quad (19)$$

The first-order rate constant k_{obsd} for the diethyl derivative of B increased slightly in proceeding from THF to acetone solutions. However, k_{obsd} was insensitive to salt effects using up to 0.2 M tetrabutylammonium perchlorate. Furthermore, the first-order rate constant was essentially unchanged in the presence of 0.1 M α, α' -bipyridine. For the dialkyliron(II) complexes in Table VII, the rate constant increases only slightly from the methyl to the ethyl and propyl derivatives. The iron-containing product of decomposition in eq 11 consists of an insoluble brick red precipitate derived from bis(bipyridine)iron(I) cation, as described further in the Experimental Section.

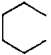
Dialkyliron(IV) Dications C. As described in eq 8 and 9 of Scheme II, the dialkyliron(IV) dications are highly unstable and can only be generated as transient intermediates in the oxidation of the dialkyliron(III) cations.^{20,21} Despite this extreme lability, C undergoes a remarkably selective extrusion of both alkyl ligands during the reductive elimination. For example, the rapid fragmentation of the labile diethyliron(IV) dication C selectively affords

(33) For hydrogen transfer by alkyl radicals after cage escape, see: Sheldon, R. A.; Kochi, J. K. *J. Am. Chem. Soc.* 1970, 92, 4395.

(34) When a half-decomposed mixture of dialkyliron(III) cations is reduced electrochemically, no scrambling of ligands is observed in the recovered A.

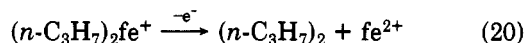
(35) Kinetics were determined in solutions typically with concentrations of 0.005 M or less in B. At higher concentrations, B is reduced to A in the course of decomposition (probably by the reduced iron(I) product). The presence of A can be readily observed by its characteristic color or by polarographic analysis.

Table VIII. Hydrocarbon Products from the Thermal Decomposition of the Dialkyliron(IV) Dication C^a

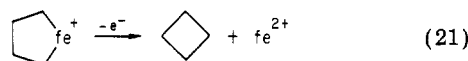
R ₂ Fe-(bpy) ₂ (ClO ₄) ₂ R (μmol)	coulometry <i>n</i> ^b	hydrocarbon, μmol		
		R ₂ (%) ^c	RH	R-H
Et (50)	1.79	38 (76)	2	~0.1
Et ^d (45)	1.80	36 (72)	4	<0.1
<i>n</i> -Pr (50)	1.88	41 (82)	6	0.4
Et (25)	1.74	22 (88) ^e	2	<0.1
<i>n</i> -Pr (25)		20 (80)	2	0.3
 (30)	1.71	24 (80)	<0.1	<0.1

^a Generated electrochemically from the oxidation of the dialkyliron(II) complex at 0.8 V in 6 mL of THF containing 0.1 M TBAP. ^b Electrons per R₂Fe(bpy). ^c Numbers in parentheses refer to % yield based on a mol of hydrocarbon produced from a mol of C. Absolute yields are minimum values, owing to losses (see Experimental Section). ^d In the presence of 600 μmol of bpy. ^e Less than 0.1 μmol of pentane detected.

butane in Table VIII. Similarly, the dipropyliron(IV) dication produces only hexane in high yields.

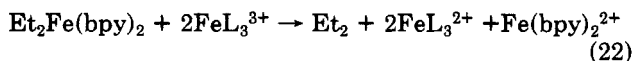


The intramolecular nature of the reductive elimination of the dialkyliron(IV) dication is demonstrated by the oxidation of an equimolar mixture of Et₂Fe(bpy)₂⁺ and *n*-Pr₂Fe(bpy)₂⁺ to give only butane and hexane, with undetectable amounts (<0.1%) of pentane, the crossover product. The ferracyclopentane cation cleanly extrudes cyclobutane upon oxidation



The iron-containing product from the decomposition of the dialkyliron(IV) dication in eq 20 consists of an insoluble red precipitate derived from bis(bipyridine)iron(II) dication, as described in further detail in the Experimental Section.

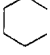
IV. Chemical Oxidation of Dialkyliron(II) Complexes. Dialkylbis(bipyridine)iron(II) also undergoes facile cleavage in the presence of chemical oxidants such as the coordinative saturated complexes of iron(III) FeL₃³⁺, where L = 1,10-phenanthroline and α,α'-bipyridine. The results in Table IX show that high yields of dialkyls (R₂) are derived from the various alkyl derivatives. Other oxidants and electrophiles such as IrCl₆²⁻, Br₂, Cl₂, I₂, ICl, Ti(O₂C-CF₃)₃, Ce(O₂CCF₃)₄, and Co(OAc)₃ were found in a previous study to have the same effect.¹⁰ Spectral titration indicated that 1.91 and 1.93 equiv of Fe(phen)₃³⁺ and Fe(bpy)₃³⁺, respectively, were consumed for each mol of Et₂Fe(bpy)₂, according to the stoichiometry



Oxidative cleavage of an equimolar mixture of Et₂Fe(bpy)₂ and *n*-Pr₂Fe(bpy)₂ produced only butane and hexane, but no crossover product, pentane (<0.1%).

The high yields of coupled alkyl products with no crossover indicate that reductive elimination is proceeding from a dialkyliron(IV) precursor C, and not the dialkyliron(III) intermediate B. Since the oxidant FeL₃³⁺ is constrained to undergo only a one-electron change,³⁶ the

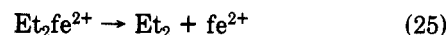
Table IX. Hydrocarbon Products from the Chemical Oxidation of Dialkyliron(II) Complexes A^a

R ₂ Fe(bpy) ₂ R (μmol)	hydrocarbon, μmol		
	R ₂ (%) ^b	RH	R-H
Me (50.0)	33 (66)	3.7	
Et (50.0)	43 (86)	3.8	<0.1
<i>n</i> -Pr (50.0)	48 (96)	1.2	<0.1
Et (25.0)	20 (80)	1.2	<0.1
<i>n</i> -Pr (25.0)			
<i>n</i> -Bu (10.0)	9.1 (91)		
 (21.4) ^d	20.4 (95) ^e	<0.1 ^f	<0.1 ^g

^a In 0.05–0.025 M solution of CH₃CN and THF with 3 equiv of Fe(phen)₃(ClO₄)₃ at 25 °C, except as stated otherwise. (See Experimental Section for details.) ^b Based on mol dialkyl per mol dialkyliron(II) complex. ^c Less than 0.1 μmol of pentane. ^d 0.01 M. ^e Cyclobutane. ^f Butane. ^g Butene.

formation of the dialkyliron(IV) dication must result from two successive oxidations, i.e., Scheme III, in which the

Scheme III



second electron-transfer step in eq 24 is faster than the reductive elimination of the dialkyliron(III) intermediate. The second-order kinetics also indicate that the initial electron transfer in eq 23 is the rate-limiting step in Scheme III. The facile oxidation of dialkyliron(III) cations by FeL₃³⁺ in eq 24 could also be demonstrated independently. Thus the oxidation of the electrochemically generated diethyliron(III) cation Et₂Fe(bpy)₂⁺ by Fe(phen)₃³⁺ afforded high yields of butane accompanied by only minor amounts (<1%) of ethane. Likewise, the di-*n*-propyl and ferracyclopentyl cations produced excellent yields (>90%) of hexane and cyclobutane, respectively, upon oxidation with Fe(phen)₃³⁺.

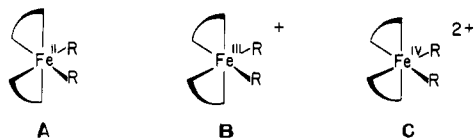
Discussion

X-ray crystallography and ¹H NMR spectroscopy have unambiguously established the structure of dialkylbis(α,α'-bipyridine)iron(II) complexes A to exist in the *cis* configuration, both in the solid and in solution. Transient electrochemical techniques as well as electron spin resonance studies also establish the one-electron oxidation of A to the dialkylbis(bipyridine)iron(III) cation B to occur with essentially no skeletal changes.³⁷ Analysis of the sweep dependence of the cyclic voltammetric wave indicates that the irreversible one-electron oxidation of the cation B generates a highly metastable dialkylbis(bipyridine)iron(IV) dication C by a rate-limiting electron transfer. The facile reductive elimination of the pair of alkyl ligands selectively to dialkyls strongly suggests that the dication C also exists in a *cis* configuration. In other words, the oxidation of A proceeds by successive one-electron transfers to afford a series of three isomeric organometallic species whose principal difference lies in the different oxidation states of the metal center,³⁸ i.e., A, B, and C. In these *cis* dialkyliron species the juxtaposition of the alkyl ligands represents an optimal condition for facile reductive elimination to occur.³⁹

(36) Dulz, G.; Sutin, N. *Inorg. Chem.* **1963**, *2*, 917. Diebler, H.; Sutin, N. *J. Phys. Chem.* **1964**, *68*, 174. Wilkins, R. G.; Yelin, R. E. *Inorg. Chem.* **1968**, *7*, 2667.

(37) For a discussion, see footnote 17.

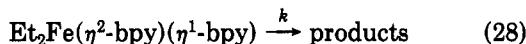
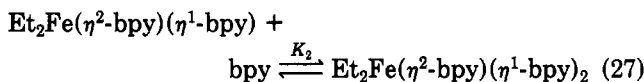
(38) Variations in bond lengths attendant upon changes in the oxidation states are not included in this consideration.



I. Mechanisms of Reductive Elimination of Dialkyliron Species A, B, and C. We now direct our attention to how each of the dialkylbis(bipyridine) analogues of iron(II), iron(III), and iron(IV) undergoes reductive elimination by a unique pathway.

Dialkyliron(II) Complex A. Earlier, Yamamoto and co-workers ascribed the retardation of the rate of decomposition of the diethyliron(II) complex A by added α, α' -bipyridine to the equilibrium in eq 27 of Scheme IV.²⁴

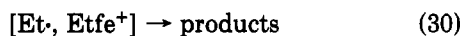
Scheme IV



According to Scheme IV, the coordinatively unsaturated intermediate is free in eq 28 to produce ethylene and ethane via β -elimination followed by hydrogen transfer.⁴⁰ Indeed this sequence of reactions leading to reductive elimination has been established in a variety of organometallic systems which are known to proceed via a dissociative mechanism.⁴¹⁻⁴⁴

Dialkyliron(III) Cations B. The rate of the thermal decomposition of dialkyliron(III) cations (Table VII) is essentially unaffected by the presence of added α, α' -bipyridine. This kinetic behavior contrasts with that of the iron(II) analogue described above, and it indicates that the dialkyliron(III) cation undergoes reductive elimination via a nondissociative mechanism. Coupled with the experimental evidence (presented in Table V, eq 16, and Figure 7) for the formation of alkyl radicals as prime intermediates, a homolytic fragmentation is the preferred pathway for the decomposition of dialkyliron(III) cations (Scheme V, where $\text{fe} = (\text{bpy})_2\text{Fe}$). According to the mechanism in

Scheme V



Scheme V, the cleavage of an alkyl-iron bond initially generates a radical ion pair, indicated in brackets. This homolysis may be followed in rapid succession by the cleavage of the second alkyl-iron bond. Cage combination

(39) The C-Fe-C bond angle in diethylbis(bipyridine)iron(II) is 85° , and the C-C bond distance between the α -carbons of the ethyl ligands is only 2.79 Å.

(40) Although such a mechanism may play an important role in the decomposition of A, other processes must also be included to account for the substantial amounts of extra alkane (i.e., alkane in excess of alkene) commonly observed (see Table IV). However, the singular absence of the coupled dialkyls from the ethyl, *n*-propyl, and *n*-butyl derivatives, as well as cyclobutane from the ferracyclopentane, indicate that significant concentrations of alkyl radicals are not involved.

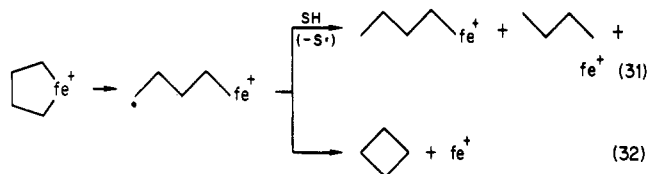
(41) For β -elimination in an alkyl-iron organometal, see: Reger, D. L.; Culbertson, E. C. *Inorg. Chem.* 1977, 16, 3104.

(42) Whitesides, G. M.; Gaasch, J. F.; Stedronsky, E. R. *J. Am. Chem. Soc.* 1972, 94, 5258.

(43) Ikariya, T.; Yamamoto, A. *J. Organomet. Chem.* 1976, 120, 257.

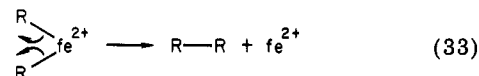
(44) For a summary discussion, see ref 8, pp 247-258.

and disproportionation of the fragments affords the mixture of alkanes and alkenes listed in Table V.⁴⁵ Diffusive separation of the alkyl radical from the solvent cage is responsible for the effects of scavengers such as nitrosodurene and acetone- d_6 . Furthermore, the formation of cyclobutane and butane from the ferracyclopentane cation accords with the competition shown in eq 31 and 32.⁴⁶

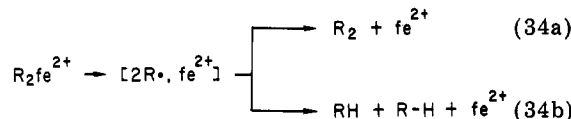


The absence of 1-butene is noteworthy, especially in comparison with its importance in the decomposition of the neutral dialkyliron(II) complex (vide supra).

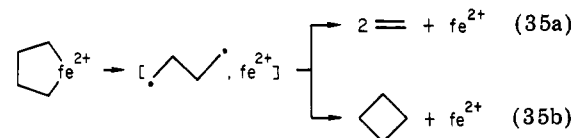
Dialkyliron(IV) Dications C. The facile reductive elimination from the metastable dialkyliron(IV) dication occurs too rapidly to carry out rigorous kinetic studies. Nonetheless, the absence of an observable effect of added bipyridine supports a nondissociative process for the reductive elimination.⁴⁷ In such a mechanism, the selective loss of dialkyl without significant competition from disproportionation (i.e., the formation of alkane and alkene) indicates that both alkyl bonds to the iron center in C are cleaved simultaneously, as in a concerted electrocyclic process.



An alternative mechanism involves the homolytic fragmentation of both alkyl-iron bonds (either simultaneously or in rapid succession) to afford a radical pair. The latter mechanism is disfavored for two reasons: (a) the radical pair should afford a mixture of alkane and alkene in addition to dialkyl from cage disproportionation and recombination known to occur according to eq 34⁴⁸ and (b) the



ferracyclopentane dication should yield ethylene in addition to cyclobutane, according to the established behavior of the tetramethylene diradical,⁴⁹ i.e., eq 35.



(45) The fate of the $\text{EtFe}(\text{bpy})_2^+$ fragment will depend on the second Fe-C bond energy, as described in the decomposition of dialkylmercury compounds [Benn, R. *Chem. Phys.* 1976, 15, 369 and ref 8, Chapter 11]. There is insufficient evidence at this juncture to evaluate this point. However, the evidence for the cage reactions of ethyl radicals points to a fast second homolysis. It is also possible that disproportionation and combination results from the direct collapse of the radical cation pair in eq 30.

(46) Small amounts of ethylene have also been observed in the decomposition of the ferracyclopentane cation.

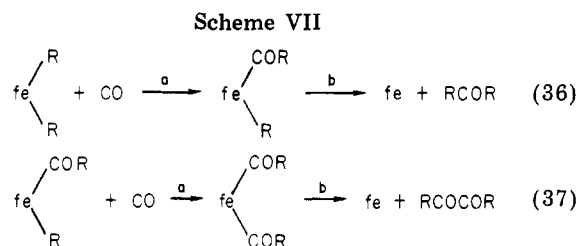
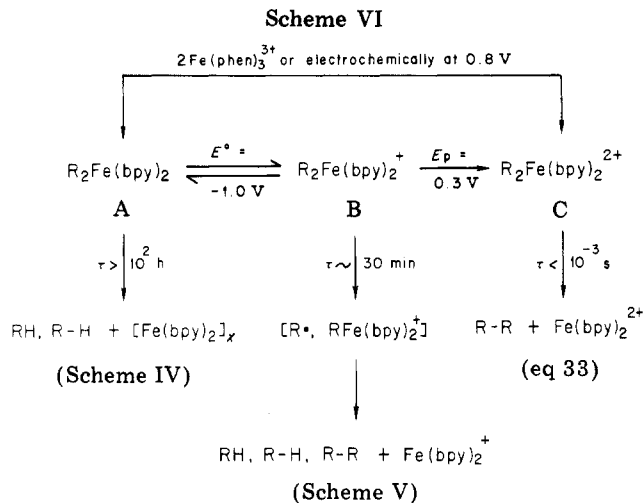
(47) (a) The first-order rate of conversion of a η^2 -bipyridine to η^1 -bipyridine in eq 26 has been measured by Yamamoto and co-workers²⁴ to be $k_1 = 0.21 \text{ min}^{-1}$. If so, it is too slow to accommodate the incorporation of bpy on the electrochemical time scale of milliseconds or less for the fragmentation in eq 33 to occur. Electrochemical oxidation of A at 0.8 V is unaffected by added α, α' -bipyridine. (b) It is unlikely that reductive elimination of alkyl ligands is simultaneous with electron transfer. See ref 20 and 21.

(48) The radical pair in eq 34 is considered to be equivalent to that in eq 13.

The different pathways outlined in Schemes IV and V and in eq 33 for the reductive elimination of various dialkyliron species underscore the critical role of the oxidation state in influencing the course of reductive elimination.

II. Comparative Behavior of Organoiron(II), -iron(III), and -iron(IV) Analogues. The comparisons of reductive elimination reveal the distinctive behavior among the dialkyliron analogues A, B, and C in two principal ways. First, the rates of cleavage of the alkyl-iron bonds vary markedly with the oxidation state of the iron center. For example, the half-life for reductive elimination in the series of diethyl analogues of A, B, and C is $\tau \geq 15$ days, 38 min, and $<10^{-3}$ s, respectively, at 30 °C. Second, the cleavage of the alkyl-iron bonds in each of these species proceeds by a characteristic mechanism. Thus the pathway in Scheme IV by which the neutral iron(II) derivative A undergoes reductive elimination requires coordinative unsaturation at the iron center to accommodate β -elimination of the alkyl ligand.⁵⁰ On the other hand, the less stable iron(III) cation B suffers spontaneous loss of an alkyl ligand by homolytic rupture in Scheme V. Finally, the highly metastable iron(IV) species C rejects both alkyl ligands simultaneously in eq 33.

The loss of alkyl ligands in these dialkyliron species corresponds to an overall reductive process. Although we have not measured the thermochemical change in each of these systems, the large differences in electrode potentials in Table II provide qualitative indications that the driving force for reductive elimination increases in the order $A < B < C$. On this basis alone, we would conclude that reductive elimination by a disproportionation of alkyl ligands in the neutral A represents the most energetic pathway. At the other extreme, reductive elimination by the coupling of alkyl ligands in the dication C represents the least energetic pathway. Homolytic cleavage of the cation B would then represent an intermediate situation. In other words, there is an apparent trend for both the rate and the mechanism of reductive elimination to be directly tied to the driving force. Factors which decrease the electron density at the metal center would provide an increasing stimulus for the mechanism of the reductive elimination of alkyl ligands to evolve progressively from β -elimination in the neutral A, to homolytic scission in the cation B, to the concerted coupling in the dication C. Thus when the driving force for reductive elimination (as in C) far exceeds that required for the creation of an open coordinate site (as in A), the concerted process will be favored. Such a scenario raises the interesting question of whether the diversity of pathways, which have been observed for reductive eliminations of a variety of organometallic systems,⁵² are generally dependent on such factors. Clearly a more complete theoretical treatment of this trend from a detailed orbital analysis⁵³ of the available pathways is



desirable, and we hope these studies will stimulate such an undertaking.

Summary and Conclusions

Dialkylbis(α, α' -bipyridine)iron(II) complexes A are electrochemically oxidized by successive one-electron transfers to the dialkyliron(III) cation B and the dialkyliron(IV) dication C. The isomeric A, B, and C differ principally in their oxidation states, all of them having the pair of alkyl ligands in a cis configuration. Reductive eliminations from these isomeric species proceed by the unique pathways schematically summarized in Scheme VI.

The importance of the oxidation state of an organometal in determining the reactivity and the course of reaction is also shown in some preliminary experiments⁵⁴ we wish to describe in connection with the carbonylation of the dialkyliron species A and B. For example, the exposure of either the diethyl- or the di-*n*-propyl derivative of the iron(II) complex A to 1 atm of carbon monoxide leads to gas uptake over a course of 5 h at 0 °C in THF solution. The same carbonylation of the corresponding iron(III) cations B is complete in less than 1 h. Furthermore, the organic products provide an interesting contrast between dialkyliron(II) and dialkyliron(III) behavior. Thus, A affords a mixture of ketone [Et_2CO , $n\text{-Pr}_2\text{CO}$] and diketone [$(\text{EtCO})_2$ and $(n\text{-PrCO})_2$] in high yields. Such products of organometal carbonylation are accounted for by the usual formulation involving CO insertion,⁵⁵⁻⁵⁷ followed by reductive elimination, as depicted in Scheme VII. According to Scheme VII the relative amounts of ketone to diketone are determined in the competition for the monoacyl intermediate $\text{fe}(\text{COR})\text{R}$ by reductive elimination in eq 36b and CO insertion in eq 37a. Consistent with this formulation, the yield of diketone is found to increase at the expense of ketone, as the temperature of the reaction

(49) Dervan, P. B.; Santilli, D. S. *J. Am. Chem. Soc.* **1980**, *102*, 3863. The tetramethylene diradical has been shown to undergo competitive cyclization to cyclobutane and fragmentation to ethylene with a relative rate $k_{\text{cycl}}/k_{\text{frag}} \approx 0.5$, which is relatively temperature independent (private communication from P.B.D.).

(50) A requirement for β -elimination of an alkylmetal is considered to be coordinative unsaturation at the metal center.⁵¹

(51) (a) Wilkinson, G. *Pure Appl. Chem.* **1972**, *30*, 627. (b) Braterman, P. S.; Cross, R. *J. Chem. Soc. Rev.* **1973**, *2*, 271.

(52) Reductive eliminations have been identified as reductive coupling (i.e., dialkyl formation) and reductive disproportionation (i.e., alkane and alkene formation). Reductive coupling is favored in some organometals and reductive disproportionation in other. For a review of these processes, see ref 4 (Chapter 4), ref 8 (Chapters 12 and 13), and ref 51b.

(53) As a recent example, see: McKinney, R. J.; Thorn, D. L.; Hoffmann, R.; Stockis, A. *J. Am. Chem. Soc.* **1981**, *103*, 2595, and references therein.

(54) Lau, W., unpublished results.

(55) Wojcicki, A. *Adv. Organomet. Chem.* **1973**, *11*, 87.

(56) Bryndza, H. E.; Bergman, R. G. *J. Am. Chem. Soc.* **1979**, *101*, 4766. Theopold, K. H.; Bergman, R. G. *Ibid.* **1980**, *102*, 5694.

(57) Yamamoto, T.; Kohara, T.; Yamamoto, A. *Chem. Lett.* **1976**, 1217.

is lowered from 25 to 0 °C. By contrast, the dialkyliron(III) cation B under the same conditions affords only mono-ketone. No diketone is observed (<5%), even at 0 °C, indicating that the monoacyliron(III) cationic intermediate is too transient to be intercepted by a second carbon monoxide.

A similar difference in behavior between dialkyliron(II) and dialkyliron(III) species A and B is shown toward olefins.⁵⁴ For example, it is worth emphasizing that a reduction potential E^0 of -1.0 V for the dialkylbis(bipyridine)iron(II) complex in Table II represents a sizeable driving force for oxidation. As such, even electron-deficient olefins such as maleic anhydride are sufficient electron acceptors to effect ready oxidation to the dialkyliron(III) cations.⁵⁴ It is thus not surprising that the diethyliron(III) cation is formed in greater than 80% yield when simply treated with proton sources such as trifluoroacetic acid at -78 °C. The latter emphasizes the ease with which electron transfer occurs from these organometals, even with conventional electrophiles. It underscores the caution which must be exercised in mechanistic formulations based on stoichiometry alone.

Experimental Section

Materials. Trialkylaluminum compounds were purchased from Texas Alkyl and used without further purification. $\text{Fe}(\text{acac})_3$ was prepared from $\text{FeCl}_3 \cdot 6\text{H}_2\text{O}$ and 2,4-pentanedione in H_2O in the presence of urea.⁵⁸ Et_4NClO_4 , $n\text{-Bu}_4\text{NClO}_4$, and anhydrous NaClO_4 were obtained from G. F. Smith Chemical Co. and used without further purification. $\text{Fe}(\text{phen})_3(\text{ClO}_4)_3$ and $\text{Fe}(\text{bpy})_3(\text{ClO}_4)_3$ were prepared as described previously.²¹ Nitrosodurene⁵⁹ and azoethane⁶⁰ were synthesized according to the literature methods. Alkyl lithium reagents were prepared from the corresponding alkyl chlorides in either pentane, hexane, or toluene, and they were assayed by titration with *sec*-butyl alcohol and a phenanthroline indicator.⁶¹

Benzene- d_6 and acetone- d_6 from Stohler Isotope Chemicals were first degassed by successive freeze-pump-thaw cycles, vacuum transferred to flasks containing a small amount of $\text{Et}_2\text{Fe}(\text{bpy})_2$, stirred for about 15 min, and then vacuum transferred into Schlenk flasks. All solvents were distilled and stored under argon. Reagent grade THF from Mallinckrodt Chem. Co. was first distilled from Na/K, followed by another distillation from benzophenone ketyl, and then a third distillation in which only the middle fraction (50%) was collected. THF under strong reducing conditions (e.g., Na/K) produced a substantial amount of ethylene, which necessitated the third distillation. Reagent grade ether, pentane, and hexane were distilled from benzophenone ketyl. 1,4-Dioxane and toluene were refluxed over Na/K overnight and distilled. Reagent grade acetone was distilled without additive, and only the middle cut (50%) was retained. Reagent grade acetonitrile from Mallinckrodt Chem. Co. was purified by a modification of a standard procedure.⁶² After fractional distillation from CaH_2 , the solvent was stirred with 10 g L^{-1} each of KMnO_4 and anhydrous Na_2CO_3 for 24 h. The mixture was filtered and flash distilled by using a rotovap equipped for continuous feed. It was then redistilled at high reflux ratios, first from P_2O_5 and then from CaH_2 . α, α' -Bipyridine was obtained from Aldrich Chem. Co. and recrystallized in EtOH.

All benchtop operations were carried out under an atmosphere of argon with Schlenk glassware. The flasks were first evacuated, flame dried, and refilled with argon. Solutions and solvents were transferred with the aid of hypodermic syringes which were thoroughly flushed with argon.

Synthesis of Dialkylbis(bipyridine)iron(II) with Trialkylalanes. The synthesis of the methyl, ethyl, and *n*-propyl

analogues of A was carried out according to the method developed by Yamamoto and co-workers.¹³ All manipulations were performed under an atmosphere of argon. In a typical procedure, Et_3Al (4.16 g, 36.5 mmol) was dissolved in 15 mL of hexane, the solution chilled to -78 °C, and EtOH (2.13 mL, 36.5 mmol) added dropwise with the aid of a hypodermic syringe, each addition being accompanied by a vigorous evolution of gas. The contents were transferred by syringe to a suspension of $\text{Fe}(\text{acac})_3$ (4.55 g, 12.9 mmol) and α, α' -bipyridine (4.75 g, 30.4 mmol) in ether at -20 °C. No reaction was observed with the slightly orange solution at this temperature. The mixture was allowed to slowly warm to 0 °C over a period of 2 h with stirring and then stirred overnight, during which time the ice bath melted. The black solid was removed from the deep blue solution by filtration under argon, washed three times with 15-mL aliquots of ether, followed by three washes with hexane, and dried in vacuo. The solid can be recrystallized by dissolution in toluene, followed by the addition of hexane and cooling to -20 °C over a 24-h period. The material obtained in this manner is microcrystalline. Repeated attempts to grow larger crystals under varying conditions of solvent, temperature, etc. were unsuccessful. Anal. Calcd for $\text{FeC}_{24}\text{H}_{26}\text{N}_4$: C, 67.61; H, 6.15; N, 13.14. Found: C, 66.92; H, 6.36; N, 12.88. Mol wt calcd: 426.33. Found: 450 ± 25 (cryoscopic in benzene). A similar procedure was used to prepare $\text{Me}_2\text{Fe}(\text{bpy})_2$ and $n\text{-Pr}_2\text{Fe}(\text{bpy})_2$ from commercially available Me_3Al and $n\text{-Pr}_3\text{Al}$.

The single crystal required for X-ray crystallography (see Figure 1) was grown in the following manner. The heterogeneous mixture consisting of $\text{Fe}(\text{acac})_3$, Et_2AlOEt , and α, α' -bipyridine was prepared as described above and allowed to sit in a bath maintained at -10 °C for 2 days without stirring. Under these conditions, $\text{Et}_2\text{Fe}(\text{bpy})_2$ crystallized out slowly as a heavy mass of black crystals.

Synthesis of Dialkylbis(bipyridine)iron(II) from Alkyl-lithium and Grignard Reagents. Dichlorobis(bipyridine)iron(II) was prepared by the sublimation of bipyridine from the easily prepared $(\text{bpy})_3\text{FeCl}_2$, as described by Basolo and Dwyer.⁶³ $\text{Cl}_2\text{Fe}(\text{bpy})_2$ was alkylated under argon with various alkyl lithium reagents; a typical procedure is described for $\text{Et}_2\text{Fe}(\text{bpy})_2$ as follows. $\text{Cl}_2\text{Fe}(\text{bpy})_2$ (2.0 g, 4.6 mmol) was suspended in 30 mL of toluene at -78 °C, and a solution of EtLi (23 mL of 0.2 M solution in toluene) was added slowly over the course of 10 h. A deep blue solution was formed, and the solution was allowed to warm slowly to room temperature after all the EtLi was added. After the mixture was stirred for 1 h at room temperature, the LiCl was removed by filtration and the solvent pumped off in vacuo. The black (deep blue) solid was washed with ether several times and recrystallized from a mixture of toluene and hexane. $\text{Et}_2\text{Fe}(\text{bpy})_2$ prepared by this procedure was comparable to that synthesized from Et_3Al and found to have the same ^1H NMR spectrum and electrochemical behavior. Acidolysis of a 1-mL THF solution of 0.05 M $\text{Et}_2\text{Fe}(\text{bpy})_2$ with a solution of sulfuric acid diluted in CH_3CN at 25 °C afforded ethane (87.7 μmol) and butane (4.3 μmol), to account for 96% of the ethyl ligands. Chemical oxidation with $\text{Fe}(\text{phen})_3(\text{ClO}_4)_3$ (3 equiv) afforded ethane (4.9 μmol) and butane (42.4 μmol), to account for 91% of the ethyl ligands. Mol wt: 472 ± 25 (cryoscopic in benzene). The ^1H NMR spectrum of $\text{Et}_2\text{Fe}(\text{bpy})_2$ was recorded on a Varian HR 220 spectrometer with a frequency sweep option and a single radiofrequency decoupler. Spectra were recorded in benzene- d_6 solutions containing a few milligrams of zinc dust and were signal averaged. The 220-MHz ^1H NMR spectrum of $\text{Et}_2\text{Fe}(\text{bpy})_2$ showed three sets of resonances at δ 0.56 (t, $J = 7$ Hz, 3 H), 1.95 (quintet, $J = 7$ Hz, 1 H), and 2.23 (quintet, $J = 7$ Hz, 1 H) for the ethyl ligands and a typical set of aromatic resonances between δ 6.0 - 9.5 for the bipyridine ligands. Decoupling at either 220 032 598 or 220 032 536 Hz (corresponding to δ 2.23 or 1.95, respectively) led to the collapse of the triplet resonance at δ 0.56 to a doublet (7 Hz). Decoupling at either 220 032 567 Hz (corresponding to the center of the two sets of quintets at δ 2.09) led to the collapse of the triplet at δ 0.56 to a singlet. Finally, decoupling at 220 032 229 Hz (corresponding to δ 0.56) led to the collapse of the pair of quintets to a pair of doublets (8 Hz) without altering their splitting of 62 Hz.

(58) Cf. Steinbach, J. F.; Burns, J. H. *J. Am. Chem. Soc.* 1958, 80, 1839.

(59) Smith, L. I.; Taylor, F. L. *J. Am. Chem. Soc.* 1935, 57, 2370, 2460.

(60) Renaud, R.; Leitch, L. C. *Can. J. Chem.* 1954, 32, 545.

(61) Watson, S. C.; Eastham, J. F. *Organomet. Chem.* 1967, 9, 165.

(62) O'Donnell, J. F.; Ayres, J. T.; Mann, C. K. *Anal. Chem.* 1965, 37, 1161.

(63) Basolo, F.; Dwyer, F. P. *J. Am. Chem. Soc.* 1954, 76, 1454.

$n\text{-Bu}_2\text{Fe}(\text{bpy})_2$ was synthesized from $\text{Cl}_2\text{Fe}(\text{bpy})_2$ suspended in toluene and $n\text{-BuLi}$ in hexane, as described above. However, no reaction was observed at -78°C even after $\sim 20\%$ of the BuLi was added. When the temperature was raised to -45°C , the blue color of the dialkyliron(II) complex was apparent. The remainder of the BuLi was added at this temperature and the workup carried out as described above.

Attempts to prepare $i\text{-Pr}_2\text{Fe}(\text{bpy})_2$ from $\text{Cl}_2\text{Fe}(\text{bpy})_2$ in toluene and $i\text{-PrLi}$ in hexane were unsuccessful. The characteristic deep blue solution of the dialkylbis(bipyridine)iron(II) complex was formed at -50°C . However, the complex slowly decomposed at -20°C over a course of several days to afford a mixture consisting of dark red solution and a red precipitate. The latter is diagnostic of the decomposition of $i\text{-Pr}_2\text{Fe}(\text{bpy})_2$. Analysis of the gas phase over the mixture indicated the presence of propane and propylene in more or less equimolar amounts. Similarly, a mixture of $\text{Cl}_2\text{Fe}(\text{bpy})_2$ and $i\text{-BuLi}$ in toluene afforded a deep blue solution which was stable at -20°C . However, it decomposed to a reddish brown solution when allowed to warm to room temperature. The analysis of the gas phase indicated a roughly 2:1 ratio of isobutane and isobutylene.

A mixture of $\text{Cl}_2\text{Fe}(\text{bpy})_2$ in toluene and $s\text{-BuLi}$ in cyclohexane also afforded a deep blue solution of the putative $s\text{-Bu}_2\text{Fe}(\text{bpy})_2$. The solution degraded to a reddish mixture upon standing overnight at -20°C . A similar reaction of $\text{Cl}_2\text{Fe}(\text{bpy})_2$ in toluene and neopentyl lithium in pentane only darkened on mixing at -20°C . The blue color characteristic of a dialkyliron(II) complex was not observed.

Synthesis of the ferracyclopentane $\overline{\text{CH}_2\text{CH}_2\text{CH}_2\text{CH}_2\text{Fe}(\text{bpy})_2}$ from the 1,4-dithiobutane, as described above, afforded only an impure product. An alternate route from the Grignard reagent was carried out as follows. 1,4-Dibromobutane (16.7 mmol) was treated with triply sublimed Mg (0.9 g, 37 mmol) in 40 mL of ether. After being refluxed for 2 h, the mixture separated into two layers. Addition of 40 mL of THF led to a colorless precipitate which was removed by filtration. The colorless solution containing the di-Grignard reagent (41 mL, 0.05 M) was added slowly with constant stirring to a suspension of $\text{Cl}_2\text{Fe}(\text{bpy})_2$ (1.2 g, 2.7 mmol) in 40 mL of 1,4-dioxane at room temperature. After the mixture was stirred for an additional 2 h, the solid was filtered, and the solution concentrated in vacuo. The solution was chilled to -20°C , and the frozen mixture was freeze-dried in vacuo. The fluffy powder was washed twice with 20-mL portions of hexane and extracted twice with 40-mL portions of ether. Removal of the ether in vacuo afforded a black solid, which was recrystallized from a mixture of toluene and hexane. Anal. Calcd for $\text{FeC}_{28}\text{H}_{32}\text{N}_4\text{O}_2$ ($\overline{\text{CH}_2\text{CH}_2\text{CH}_2\text{CH}_2\text{Fe}(\text{bpy})_2$, 1,4-dioxane): C, 65.61; H, 6.31; N, 10.93. Found: C, 65.46; H, 6.29; N, 10.95. Mol wt calcd: 424.33. Found: 493 ± 25 (cryoscopic in benzene). The proton ^1H NMR spectrum of the ferracyclopentane in benzene- d_6 consists of two sets of unresolved resonances at δ 1.11 (4 H) and δ 1.49 (4 H), in addition to the bpy resonances (16 H).

Decomposition of Dialkylbis(bipyridine)iron(II). The decompositions of the dialkylbis(bipyridine)iron(II) complexes were carried out in sealed glass tubes in vacuo. In a typical experiment, a 1-mL aliquot of a 0.05 M solution of $\text{Et}_2\text{Fe}(\text{bpy})_2$ in THF was introduced under argon at 25°C into a 25-mL bulb with a glass stem connected to a Schlenk adaptor. The bulb was evacuated and the tube sealed at liquid-nitrogen temperatures. After thermal decomposition at 50°C , a rubber tubing was fitted tightly over the glass tube extension which was then broken at the preengraved scratch mark. The bulb was filled with argon with the aid of a syringe needle and an appropriate internal standard added. [Note: In a separate experiment, the gases were analyzed prior to the addition of the internal standard.] The hydrocarbons were analyzed by gas chromatography using the following columns: 2 ft Porapak Q for CH_4 , C_2H_4 , and C_2H_6 ; 15 ft DBTCP for C_3 and C_4 hydrocarbons; 10 ft Carbowax 5M for C_5 and C_6 hydrocarbons; and 6 ft FFAP for C_8 hydrocarbons. Standard calibration curves were constructed for each component under the reaction conditions. For the ferracyclopentane decomposition, the evolution of butane and 1-butene was continuously monitored throughout the reaction but showed no variation from the start to the end. Furthermore, the product composition of a thermolysis at 90°C was unchanged (C_4H_{10} , 17.3 μmol , and C_4H_8 ,

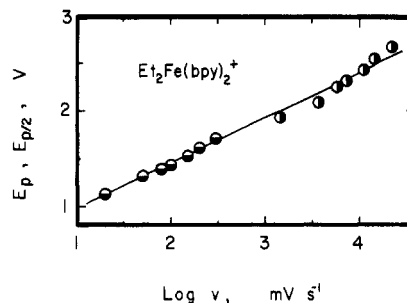


Figure 8. Variation of the anodic peak potential E_p (●) and $E_{p/2}$ (■) on the CV sweep rate ($\log v$) for W_2 of 0.003 M $\text{Et}_2\text{Fe}(\text{bpy})_2$ in acetone containing 0.1 M TEAP at 0°C . The value of E_p has been shifted by adding 1.857 to $\log v$.

13.6 μmol) relative to that formed at 50°C (see Table IV).

Electrochemical Measurements. Electrochemistry was performed on a Princeton Applied Research Model 173 potentiostat equipped with a Model 176 current-to-voltage converter which provide a feedback compensation for ohmic drop between the working and reference electrodes. The voltage follower amplifier (PAR Model 178) was mounted external to the potentiostat with a minimum length of high impedance connection to the reference electrode. This arrangement ensured low noise pickup. Cyclic voltammograms were recorded on a Houston series 2000 X-Y recorder. The electrochemical cell was constructed according to the design of van Duyne and Reilly.⁶⁴ The distance between the platinum working electrode and the tip of the salt bridge was 1 mm to minimize ohmic drop. Coulometry was carried out by using a three-compartment cell of conventional design with a platinum gauze electrode. A special cell was constructed with an additional sidearm to accommodate an extra electrode in order to conveniently monitor the solution by cyclic voltammetry at anytime during an oxidation or reduction. This can be done by simply switching the connection between the two working electrodes and leaving all other connections intact. The optimum cyclic voltammogram was obtained with a configuration in which the CV working electrode was located directly opposite to the reference electrode. All operations were performed under an atmosphere of argon. A 0.2 M solution of $n\text{-Bu}_4\text{NClO}_4$ was used as supporting electrolyte with THF, and a 0.1 M solution of Et_4NClO_4 or NaClO_4 was used with acetone and acetonitrile. Electrolyses were carried out at 0°C to minimize decomposition of either A or B. The time required for the complete oxidation of 0.1 mmol of $\text{Et}_2\text{Fe}(\text{bpy})_2$ at -0.35 V and 0°C was $\sim 5\text{--}10$ min in acetone and about 30 min in THF. Analysis of the gas phase showed minimal decomposition under these conditions. The coulometric current was stored in a Princeton Applied Research Model 4102 signal recorder for later output onto a Leed and Northrup Speedomax strip chart recorder. When the green solution after the electrolysis was transferred immediately to a Schlenk flask and stored at -78°C under argon, no decomposition was observed.

Electrochemical irreversibility of the CV wave W_2 for $\text{Et}_2\text{Fe}(\text{bpy})_2$ was determined by the procedure outlined earlier.¹¹ First the plot of E_p or $E_{p/2}$ against the sweep rate ($\log v$) shown in Figure 8 yields slopes greater than 30 mV/decade, indicating that the electron-transfer step is not reversible. Second, the transfer coefficient β obtained from the sweep dependence (0.56) is consistent with β determined from the shape of the CV wave (0.51).^{11a} The error associated with this analysis is described in detail in ref 11b.

Decomposition of Dialkylbis(bipyridine)iron(III) Cations. A 0.05 M solution of dialkylbis(bipyridine)iron(II) in acetone or THF containing the appropriate supporting electrolyte (vide supra) was electrochemically oxidized at -0.35 V and 0°C . The green solutions of the dialkylbis(bipyridine)iron(III) cation were stored in a Schlenk flask under argon at -78°C . The solutions were assayed by oxidation with $\text{Fe}(\text{phen})_3^{3+}$ and quantitative analysis of the hydrocarbon products. The solutions were diluted 10-fold to 0.005 M prior to decomposition, as described in the

foregoing section. The effect of electrolyte was examined by the deliberate addition of various amounts of salt.

The formation of alkane in the thermal decomposition of dialkyliron(III) cations was examined in acetone- d_6 . Typically, a 0.03 M solution of $\text{Et}_2\text{Fe}(\text{bpy})_2$, consisting of 6 mL of acetone- d_6 and containing 0.1 M NaClO_4 , was oxidized at -0.35 V and 0 °C. [The counterelectrode compartment also contained acetone- d_6 to avoid complications from diffusion.] A 1-mL aliquot was diluted with 3 mL of acetone- d_6 , sealed in a glass ampule, and decomposed at 30 °C. The hydrocarbons consisted of C_2H_4 (2.5 μmol), C_2H_6 (10.3 μmol), and $n\text{-C}_4\text{H}_{10}$ (8.0 μmol) or a 95% total yield of ethyl groups (based on the $\text{Fe}(\text{phen})_3^{3+}$ oxidation of a second 1-mL aliquot). The mass spectral cracking pattern at 70 eV consisted of the following: m/e (%): ethylene, 25 (13.1), 26 (59.1), 27 (63.9), 28 (100), 29 (3); ethane, 25 (5.0), 26 (24.6), 27 (34.8), 28 (100), 29 (19.7), 30 (25.4); ethane- d_1 , 25 (4.4), 26 (18.5), 27 (32.7), 28 (64.2), 29 (100), 30 (24.4), 31 (32.2). The mass spectrum of the ethane fraction from the decomposition was matched with that calculated from the known cracking patterns of C_2H_6 and $\text{C}_2\text{H}_6\text{D}$ (vide supra). The composition consisting of 72% $\text{C}_2\text{H}_6\text{D}$ and 28% C_2H_6 was the closest to the experimental spectrum, enumerated as follows: m/e , % experimental (% calculated): 25, 5.4 (5.9); 26, 23.8 (26.1); 27, 40.4 (43.0); 28, 90.6 (95.7); 29, 100 (100); 30, 30.8 (31.9); 31, 29.0 (29.9). The yield of C_2H_6 is thus 2.9 μmol , which is equivalent to the ethylene (2.5 μmol) formed in the thermolysis.

Kinetics of Dialkylbis(bipyridine)iron(III) Decomposition. The rates of decomposition of 0.005 M dialkyliron(III) cation B in THF were measured by following its disappearance spectrophotometrically at 680 nm. However, the precipitation of the iron product became serious at about 40% decomposition. Thus only the initial portion of the decay could be measured quantitatively. In order to follow the disappearance of the dialkyliron(III) cation to completion, we measured its concentration (~ 0.003 M) polarographically by monitoring the diffusion current between -0.8 and -1.2 V in acetone and THF. Under these conditions, the rate followed a first-order decay beyond 3 half-lives. The rate constants measured spectrophotometrically were the same as those obtained polarographically in the same solvent.

Electrochemical Oxidation of Dialkylbis(bipyridine)iron(II). A THF solution of 0.005 M $\text{Et}_2\text{Fe}(\text{bpy})_2$ containing 0.2 M $n\text{-Bu}_4\text{NClO}_4$ was anodically oxidized at a constant potential of 0.8 V. As the electrolysis proceeded, the deep blue solution turned dark and eventually lightened to a pink solution containing a red precipitate. The hydrocarbon products were C_2H_6 (2.1 μmol), $n\text{-C}_4\text{H}_{10}$ (38.2 μmol), and C_2H_4 (<0.2 μmol). Note that the absolute yields obtained from this type of experiment are less accurate than those carried out in sealed tubes owing to losses of material by diffusion into the counterelectrode compartment during electrolysis. Coulometry indicated that $1.79 e^-$ was liberated for each $\text{Et}_2\text{Fe}(\text{bpy})_2$. A two-step oxidation of 6 mL of 0.009 M $\text{Et}_2\text{Fe}(\text{bpy})_2$ was performed at -0.35 V, which liberated $0.89 e^-/\text{iron}$. This electrolysis was followed by oxidation at 0.8 V which liberated $0.72 e^-$ per iron. The yield of n -butane was 36.7 μmol , and the combined yield, C_2H_6 plus C_2H_4 , was 26.6 μmol . The relatively high yields of the latter arose from the partial decomposition of the dialkyliron(III) intermediate at room temperature, which also accounted for the drop in coulometry in the second step.

Photolysis of Azoethane. A 0.005 M solution of azoethane in THF was photolyzed with a medium-pressure (Hanovia, 1 kW) mercury lamp using an aqueous copper(II) sulfate filter (15 g of CuSO_4 in 100 mL). In THF solution, the absorption band of azoethane lies at 360 nm with a half-band width of ~ 40 nm. The copper sulfate filter solution lies in the region from 3650 to 3663 Å.⁶⁵ Styrene (2–5 mol%) was found to be more useful as a trap than either 1,1-diphenylethylene or α -methylstyrene, which absorb in the same region as azoethane.

ESR Measurements. All experiments were performed on a Varian E-112 spectrometer equipped with a Hewlett-Packard 5248L electronic counter and a 5255A frequency converter together with a Harvey Wells G502 gaussmeter. The samples were cooled in a quartz Dewar located in the ESR cavity with a flow of cold nitrogen. All g values are corrected relative to perylene radical ($g = 2.00257$) as the standard. The spin-trapping experiments

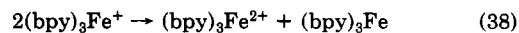
were carried out by freezing successive layers of 0.02 M nitrosodurene and 0.02 M $\text{Et}_2\text{Fe}(\text{bpy})_2^+$ dissolved in THF in a quartz ESR tube at -196 °C. The mixture was quickly warmed to room temperature with shaking and allowed to decompose in the cavity at 25 °C.

Chemical Oxidation of Dialkylbis(bipyridine)iron(II). In a typical experiment, 150 μmol of oxidant ($\text{Fe}(\text{bpy})_3(\text{ClO}_4)_3$ or $\text{Fe}(\text{phen})_3(\text{ClO}_4)_3$) was weighed into a 25-mL round-bottom flask containing a magnetic stir bar. The flask was then capped with a rubber septum and filled with argon by pumping and refilling through a syringe needle. CH_3CN (4 mL) was added, and the solution was stirred vigorously while 1 mL of a 0.05 M solution of $\text{Et}_2\text{Fe}(\text{bpy})_2$ in THF (50 μmol) was introduced with the aid of a hypodermic syringe. Cyclopropane (0.5 mL) was added as an internal standard after the reaction was complete. The content was equilibrated at 0 °C for 15 min and thoroughly mixed. The organic products were analyzed in the gas phase by gas chromatography using a 10-ft DBTCP column.

Spectral titrations were performed by adding known quantities of a stock solution of $\text{Et}_2\text{Fe}(\text{bpy})_2$ to a volumetric flask containing a known aliquot of the oxidant in excess. Reaction was complete upon mixing, after which the contents were diluted to volume. The absorption spectrum was measured on a Cary 14 spectrometer. In a typical example, 0.1 -mL aliquots of a 1.00×10^{-2} M solution of $\text{Fe}(\text{phen})_3(\text{ClO}_4)_3$ in CH_3CN were introduced into several 5-mL volumetric flasks (equipped with a serum stopper) and pre-filled with argon. Aliquots (0.14 – 0.16 mL) of a 0.05 M solution of $\text{Et}_2\text{Fe}(\text{bpy})_2$ in THF were added, and the final solutions were diluted to volume. The absorbance of $\text{Fe}(\text{phen})_3^{2+}$ (λ_{max} 507 nm (ϵ 13 000))²¹ was plotted against the amount of $\text{Et}_2\text{Fe}(\text{bpy})_2$ added, and the least-squares slope was evaluated as the equivalents of $\text{Fe}(\text{phen})_3^{3+}$ consumed per equivalent of $\text{Et}_2\text{Fe}(\text{bpy})_2$ oxidized.

Synthesis and Characterization of Tris(bipyridine)iron(II, I, 0) Complexes. The tris(bipyridine) complexes of iron ($\text{bpy})_3\text{Fe}^n$ in the oxidation states $n = +3, +2, +1$, and 0 have been identified in polarographic studies.⁶⁶ Indeed the cyclic voltammograms show reversible behavior for the one-electron couples ($\text{bpy})_3\text{Fe}^{3+}/(\text{bpy})_3\text{Fe}^{2+}$, ($\text{bpy})_3\text{Fe}^{2+}/(\text{bpy})_3\text{Fe}^+$, and ($\text{bpy})_3\text{Fe}^+ / (\text{bpy})_3\text{Fe}$ in acetonitrile solutions at $E^0 = 1.03, -1.34$, and -1.53 V vs. saturated NaCl SCE.

The iron(II) complex was readily prepared by standard methods⁶⁷ and identified in solution by its characteristic visible absorption spectrum showing a band with λ_{max} 525 nm (ϵ 8240) with a shoulder at ~ 490 nm in acetonitrile. The iron(0) complex was prepared by the electrochemical reduction of the iron(II) complex at a constant potential of -1.65 V. As the bulk electrolysis proceeded, the dark maroon red solution gradually lightened, and a dark red solid precipitated from the acetonitrile solution. Coulometry indicated that two electrons per iron were required for the reduction. Although the dark red solid is sparingly soluble in 1,2-dimethoxyethane, a saturated solution showed the same absorption bands (λ_{max} 532, 500, 358 nm) as those reported earlier for ($\text{bpy})_3\text{Fe}^0$ prepared by an alternative method.^{26b} The iron(I) complex was prepared in acetonitrile solution by the electrochemical reduction of the iron(II) complex (72 μmol) at a controlled current of 10 mA for 695 s, which corresponded to the take up of one electron per iron. The electrode potential gradually decreased from -1.35 V initially to -1.45 V at the end of the electrolysis. The dark violet red solution showed a new absorption band at 600 nm as a partially resolved shoulder off the principal double band centered at 525 and 490 nm. The cyclic voltammogram indicated the presence of a ($\text{bpy})_3\text{Fe}^+$ species which can be reversibly oxidized to ($\text{bpy})_3\text{Fe}^{2+}$. The iron(I) complex could not be isolated as a crystalline salt from solution owing to its instability, i.e., eq 38. The facile disproportionation in eq 38 can



be demonstrated in two ways. (1) On standing, the dark violet solution changed to a bright red color and deposited a brown

(65) Calvert, J. G.; Pitts, J. N., Jr. "Photochemistry", Wiley: New York, 1966, p 734.

(66) Tanaka, N.; Sato, Y. *Electrochim. Acta* 1968, 13, 335. Misono, A.; Uchida, Y.; Hidai, M.; Yamagishi, T.; Kageyama, H. *Bull. Chem. Soc. Jpn.* 1973, 46, 2769. Tanaka, N.; Ogata, T.; Niizuma, S. *Ibid.* 1973, 46, 3299.

(67) Ford-Smith, M. H.; Sutin, N. *J. Am. Chem. Soc.* 1961, 83, 1830.

Table X. Fractional Coordinates and Isotropic Thermal Parameters for $\text{Et}_2\text{Fe}(\text{bpy})_2^a$

atom	x	y	z	B_{iso} , Å ²	atom	x	y	z	B_{iso} , Å ²
Fe(1)	3617.5 (4)	3577.1 (2)	2268.7 (2)	12	C(29)	923 (3)	3465 (1)	3840 (2)	19
N(2)	1919 (2)	4263 (1)	2060 (2)	14	H(30)	10 (3)	388 (1)	105 (2)	17 (5)
C(3)	315 (3)	4242 (1)	1458 (2)	18	H(31)	-192 (4)	468 (1)	100 (2)	32 (7)
C(4)	-858 (3)	4732 (1)	1417 (2)	22	H(32)	-121 (3)	560 (1)	201 (2)	19 (5)
C(5)	-452 (3)	5291 (1)	2011 (2)	21	H(33)	153 (3)	569 (1)	302 (2)	13 (5)
C(6)	1157 (3)	5336 (1)	2611 (2)	18	H(34)	424 (3)	577 (1)	373 (2)	11 (5)
C(7)	2331 (3)	4828 (1)	2610 (2)	15	H(35)	705 (3)	566 (1)	451 (2)	12 (5)
C(8)	4090 (3)	4843 (1)	3174 (2)	15	H(36)	853 (4)	470 (1)	444 (2)	29 (6)
C(9)	4872 (3)	5384 (1)	3699 (2)	19	H(37)	714 (3)	386 (1)	357 (2)	12 (5)
C(10)	6569 (3)	5348 (1)	4167 (2)	22	H(38)	317 (3)	447 (1)	29 (2)	14 (5)
C(11)	7442 (3)	4766 (1)	4116 (2)	22	H(39)	443 (3)	461 (1)	-119 (2)	17 (5)
C(12)	6608 (3)	4251 (1)	3592 (3)	19	H(40)	677 (3)	391 (1)	-147 (2)	10 (4)
N(13)	4939 (2)	4275 (1)	3103 (2)	13	H(41)	754 (3)	312 (1)	-27 (2)	20 (6)
N(14)	4574 (2)	3736 (1)	926 (2)	12	H(42)	803 (3)	230 (1)	92 (2)	15 (5)
C(15)	4095 (3)	4193 (1)	179 (2)	15	H(43)	884 (4)	165 (1)	243 (2)	27 (6)
C(16)	4852 (3)	4271 (1)	-734 (2)	17	H(44)	756 (4)	185 (1)	404 (2)	27 (6)
C(17)	6173 (3)	3861 (1)	-912 (2)	18	H(45)	552 (3)	263 (1)	389 (2)	10 (5)
C(18)	6675 (3)	3380 (1)	-173 (2)	17	H(46)	87 (3)	297 (1)	178 (2)	18 (5)
C(19)	5869 (3)	3325 (1)	739 (2)	14	H(47)	164 (3)	307 (1)	68 (2)	15 (5)
C(20)	6335 (3)	2860 (1)	1596 (2)	13	H(48)	342 (4)	213 (1)	100 (2)	34 (7)
C(21)	7553 (3)	2374 (1)	1557 (2)	18	H(49)	276 (4)	202 (1)	216 (2)	25 (6)
C(22)	8001 (3)	1979 (1)	2432 (2)	20	H(50)	151 (4)	194 (1)	107 (2)	27 (6)
C(23)	7231 (3)	2095 (1)	3340 (2)	21	H(51)	270 (3)	277 (1)	360 (2)	16 (5)
C(24)	6006 (3)	2567 (1)	3326 (2)	18	H(52)	355 (3)	337 (1)	424 (2)	17 (5)
N(25)	5479 (2)	2949 (1)	2458 (2)	13	H(53)	7 (3)	337 (1)	326 (2)	17 (5)
C(26)	1927 (3)	2914 (1)	1459 (2)	16	H(54)	56 (3)	325 (1)	451 (2)	20 (5)
C(27)	2455 (4)	2210 (1)	1419 (3)	24	H(55)	89 (3)	392 (1)	393 (2)	23 (6)
C(28)	2695 (3)	3251 (1)	3624 (2)	17					

^a Fractional coordinates are $\times 10^4$ for nonhydrogens and $\times 10^3$ for hydrogens. B_{iso} are $\times 10$. Isotropic values for those atoms which were refined anisotropically are calculated by using the formula given by Hamilton, W. C. *Acta Crystallogr.* 1959, 12, 609.

amorphous-looking solid. The cyclic voltammogram of the bright red solution indicated it to consist solely of $(\text{bpy})_3\text{Fe}^{2+}$. The amount of the iron(II) complex formed was determined spectrophotometrically at 525 nm and found to be present in 50%, 56%, and 56% yields when starting from 72, 190, and 418 μmol of iron(I), respectively. The accompanying brown solid was isolated gravimetrically and quantitatively analyzed for its iron content by standard methods,⁶⁸ after digestion with hydrochloric acid. Approximately 40% of the original iron was contained in the brown solid. Although we did not further characterize the brown solid, we noted that similar material was derived from the iron(0) complex upon dissolution in a solvent such as tetrahydrofuran. We tentatively suggest that it is a polymeric iron(0) complex. (2) The facile disproportionation of the iron(I) complex in eq 38 is also indicated by cyclic voltammetry. Thus at low concentrations (<0.002 M), the cyclic voltammogram of $(\text{bpy})_3\text{Fe}^{2+}$ showed three reversible waves at $E^0 = 1.03, -1.34,$ and -1.53 V, which correspond to the iron(II, III), iron(II, I), and iron(I, 0) couples. At slightly higher concentrations (>0.004 M), the current for the anodic component of the wave at -1.34 V increased at the expense of that for the anodic component of the wave at -1.53 V. Indeed the iron(I, 0) wave shows the earmarks of irreversible behavior. [The iron(II, III) wave at 1.03 V was unaffected by changes in concentration.] Such a concentration dependence of the CV waves for the iron(II, I) and iron(I, 0) couples can be readily ascribed to the disproportionation of the $(\text{bpy})_3\text{Fe}^+$ which competes with its reversible oxidation, all on the CV time scale of approximately milliseconds.

Identification of the Iron-Containing Products of the Reductive Elimination of Various Dialkyl(bipyridine)iron Complexes. The synthesis and characterization of the tris(bipyridine) complexes of iron(II, I, 0) allowed the iron-containing products which were derived from the reductive elimination of the dialkyl(bipyridine)iron(IV, III, II) analogues to be readily identified. Thus the iron-containing product from dialkyl(bipyridine)iron(II), designated as *fe* in eq 10, was identified as

$(\text{bpy})_3\text{Fe}^0$ when the decomposition was carried out in the presence of added bipyridine. Similar results were observed earlier by Yamamoto and co-workers.¹⁵

The reductive elimination of the dialkyl(bipyridine)iron(III) cation affords an iron(I) species fe^+ , according to the stoichiometry given in eq 11. Indeed, when the decomposition was carried out with added bipyridine, the presence of $(\text{bpy})_3\text{Fe}^+$ could be detected from its characteristic absorption spectrum and cyclic voltammogram (vide supra). As a result of its instability, however, a quantitative analytical method could not be developed for $(\text{bpy})_3\text{Fe}^+$. Instead, the disproportionation products given in eq 38 were determined. From 37 μmol of $\text{Et}_2\text{Fe}(\text{bpy})_2^+$, the yield of $(\text{bpy})_3\text{Fe}^{2+}$ was 46 and 51%, with and without added bipyridine, respectively. Owing to the small amounts of $\text{Et}_2\text{Fe}(\text{bpy})_2^+$ involved, the brown iron(0) solid could not be accurately analyzed gravimetrically. However, we qualitatively noted that the brown iron(0) solid was formed in the decomposition of $\text{Et}_2(\text{bpy})\text{Fe}^+$ at a rate which was faster than the rate of disproportionation of $(\text{bpy})_3\text{Fe}^+$ described above. The difference in rates can be accounted for, if the disproportionation proceeds via a prior dissociation of bipyridine,⁶⁹ followed by a rapid electron transfer of the coordinatively unsaturated iron(I) species with another iron(I) complex.

The iron-containing product from the decomposition of $\text{Et}_2\text{Fe}(\text{bpy})_2^{2+}$ was collected as a red precipitate after the oxidation at 0.8 V of a solution of $\text{Et}_2\text{Fe}(\text{bpy})_2$ and bipyridine. Spectrophotometric analysis ($\lambda_{\text{max}} 525$ nm ($\epsilon_{\text{max}} 8240$)) indicated it to consist of $(\text{bpy})_3\text{Fe}^{2+}$, which accounted for 93% of the original iron, in accord with the stoichiometry for fe^{2+} in Scheme II and eq 20 and 21.

X-ray Crystallography. The diffractometer used in this study consisted of a Picker goniostat interfaced to a T1980B minicomputer with 56K words of 16 bit memory. The angle drives of the goniostat were interfaced by using Slo-Syn stepping motors and translator driver boards. The computer is programmed to operate on an interrupt basis by using a precision internal clock, and scan speeds are controlled by the pulse rate delivered to the translator driver boards. Each pulse will drive the corresponding goniostat angle 0.005°, and virtually any angular rate can be chosen. A "filter attenuator wheel", mounted on the detector arm, is positioned such that up to 20 apertures or attenuators can be automatically located in the diffraction beam path. Apertures are

(68) Kolthoff, I. M.; Sandell, E. B.; Meehan, E. J.; Bruckenstein, S. "Quantitative Chemical Analysis", 4th ed.; Macmillan: New York, 1969; p 840.

(69) The decomposition of $(\text{bpy})_3\text{Fe}$ in dimethoxyethane proceeds by dissociation of bipyridine. See ref 26b.

provided for automatic top/bottom-left/right centering of reflections, and these are utilized for both goniostat and crystal alignment. Standard "NIM-bin" electronics are used for pulse shaping and energy discrimination, and the computer-controlled timer and scaler were constructed locally. Reflection data are collected in a normal θ - 2θ scan mode with backgrounds at each extreme of the scan. A buffer is provided so that up to 4800 reflection data can be stored in the computer memory.

A liquid-nitrogen boil-off cooling system is used to maintain samples at -140 to -180 °C. The system consists of two 30-L storage Dewars to supply the dry nitrogen gas for the cold stream and concentric warm stream and a third 30-L recoiling Dewar through which the cooling gas is passed. The recoiling Dewar consists of a coil (2-m length) of copper tubing which is joined to an evacuated and silvered glass delivery tube. The delivery tube is designed to supply the cold nitrogen in a fixed position from the bottom of the χ circle. The exit nozzle is carefully streamlined to ensure a laminar flow. Thermocouples and heating wires located in the exit nozzle monitor and control the temperature. Short-term temperature fluctuation is typically ± 0.2 °C with long-term stability of ± 3 °C. Crystals are mounted on glass fibers by using a silicon grease, which remains amorphous and becomes rigid at the normal operating temperature of the system.

Data are reduced by using the equations $I = C - 0.5(t_c/t_b)(B_1 + B_2)$ and $\sigma(I) = [C + 0.25(t_c/t_b)^2(B_1 + B_2) + (pI)^2]^{1/2}$, where C is the total integrated peak count obtained in scan time t_c , B_1 and B_2 are the background counts obtained in time t_b , and p is the "ignorance factor". The function minimized in the least-squares program is $\sum w|F_o - F_c|^2$, where $w = [\sigma(F_o)]^{-2}$, and residuals are defined as $R(F) = \sum ||F_o| - |F_c|| / \sum |F_o|$ and $R_w(F) = (\sum w||F_o| - |F_c||^2 / \sum wF_o^2)^{1/2}$.

A well-formed parallelepiped of dimensions $0.18 \times 0.25 \times 0.25$ mm was chosen for the crystallographic study of $\text{Et}_2\text{Fe}(\text{bpy})_2$. The sample was cooled to -173 °C on the goniostat, and all measurements were taken at this temperature. A search of a limited hemisphere of reciprocal space located a set of reflections which could be indexed as monoclinic of space group $P2_1/n$ (alternate setting of $P2_1/c$) with cell dimensions of $a = 7.843$ (1) Å, $b = 20.682$ (4) Å, $c = 12.590$ (3) Å, and $\beta = 98.52$ (1)° at -173 °C, based on a refinement of angular data from 28 reflections. The calculated density is 1.402 g cm^{-3} for $Z = 4$.

A total of 4208 intensities were collected by using Mo $K\alpha$ radiation (graphite monochromator) in the range $6 < 2\theta < 50^\circ$ using a continuous θ - 2θ scan over a range from 1° below the calculated $K\alpha_1$ position to 1° above the calculated $K\alpha_2$ position. Eight second stationary counts were recorded at each extreme of the scan, whose rate was 3° min^{-1} . The intensities of four

reflections which were monitored after every 300 measurements showed no noticeable trends. Data were reduced in the usual manner using an ignorance factor of 0.07. Although this may seem large, a goodness of fit of 1.008 indicates that proper weighting was achieved. Of the 3566 unique intensities, 3383 were nonzero and 3085 were considered "observed", using the criteria $F > 2.33\sigma(F)$.

Positions of all nonhydrogen atoms were determined by using direct methods and Fourier techniques. Hydrogen atoms were readily located from a difference Fourier synthesis phased on the nonhydrogen parameters. Final full-matrix refinement included anisotropic thermal parameters for nonhydrogen atoms, isotropic thermal parameters for hydrogen atoms, positional parameters and an overall scale factor. The goodness of fit for the final cycle was 1.008, and the maximum shift for any parameter was less than 0.05 times the corresponding estimated error. Final residuals were $R(F) = 0.041$ and $R_w(F) = 0.042$. Positional parameters and isotropic thermal parameters are listed in Table X. The hydrogen bond distances and bond angles, the anisotropic thermal parameters, and the observed and calculated structure factors are available in Tables XI, XII, and XIII of the supplementary materials. A final difference Fourier synthesis was featureless, the largest peak being $0.45 \text{ e } \text{Å}^{-3}$.

The molecule of $\text{Et}_2\text{Fe}(\text{bpy})_2$ has near twofold symmetry, the largest deviation occurring for the C(27)-C(29) pair, where $\Delta = 0.25$ Å. Otherwise, the largest deviation is 0.09 Å. The two Fe-ethyl planes are approximately coplanar with the 2 bpy ligands, owing partially to the intramolecular contacts between the hydrogens on C(26) [C(28)] and C(3) [C(24)] which range from 2.15 to 2.26 Å.

Acknowledgment. We wish to thank K. S. Chen and R. J. Klingler for helpful discussions and the National Science Foundation for financial support.

Registry No. $\text{Me}_2\text{Fe}(\text{bpy})_2$, 79434-52-9; $\text{Et}_2\text{Fe}(\text{bpy})_2$, 79434-51-8; $(n\text{-Pr})_2\text{Fe}(\text{bpy})_2$, 79464-40-7; $(n\text{-Bu})_2\text{Fe}(\text{bpy})_2$, 79391-80-3; $(\text{CH}_2)_4\text{Fe}(\text{bpy})_2$, 79391-79-0; $\text{Me}_2\text{Fe}(\text{bpy})_2\text{ClO}_4$, 79391-78-9; $\text{Et}_2\text{Fe}(\text{bpy})_2\text{ClO}_4$, 79391-76-7; $(n\text{-Pr})_2\text{Fe}(\text{bpy})_2\text{ClO}_4$, 79391-74-5; $(\text{CH}_2)_4\text{Fe}(\text{bpy})_2\text{ClO}_4$, 79391-72-3; $\text{Et}_2\text{Fe}(\text{bpy})_2(\text{ClO}_4)_2$, 79391-70-1; $(n\text{-Pr})_2\text{Fe}(\text{bpy})_2(\text{ClO}_4)_2$, 79391-68-7; $(\text{CH}_2)_4\text{Fe}(\text{bpy})_2(\text{ClO}_4)_2$, 79409-38-4; $(\text{bpy})_3\text{Fe}$, 15388-61-1; $(\text{bpy})_3\text{Fe}^+$, 51383-17-6; $(\text{bpy})_3\text{Fe}^{2+}$, 15025-74-8; $(\text{bpy})_3\text{Fe}^{3+}$, 18661-69-3; $\text{Cl}_2\text{Fe}(\text{bpy})_2$, 15686-12-1.

Supplementary Material Available: Complete listings of hydrogen bond distances and bond angles (Table XI), anisotropic thermal parameters (Table XII), and observed and calculated structure factors (Table XIII) (25 pages). Order information is given on any current masthead page.